Agricultural Water Management 241 (2020) 106197

Contents lists available at ScienceDirect

Agricultural Water Management

journal homepage: www.elsevier.com/locate/agwat

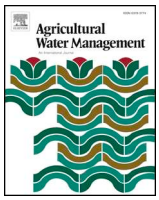

Review

Prediction of crop coefficients from fraction of ground cover and height. Background and validation using ground and remote sensing data

L.S. Pereira[a,*], P. Paredes[a], F. Melton[b,c], L. Johnson[b,c], T. Wang[b,c], R. López-Urrea[d], J.J. Cancela[e], R.G. Allen[f]

[a] LEAF- Linking Landscape, Environment, Agriculture and Food, Instituto Superior de Agronomia, Universidade de Lisboa, Tapada da Ajuda, 1349-017, Lisbon, Portugal
[b] School of Natural Sciences, California State University, Monterey Bay, Seaside, CA, 93955, USA
[c] Earth Science Division, NASA Ames Research Center, Moffett Field, CA, 94035, USA
[d] Instituto Técnico Agronómico Provincial (ITAP), Parque Empresarial Campollano, 2ª Avda. Nº 61, 02007, Albacete, Spain
[e] GI-1716, Proyectos y Planificación, Dpto. Ingeniería Agroforestal, Universidad de Santiago de Compostela, Escola Politécnica Superior de Enxeñaría, Campus Universitario s/n, 27002, Lugo, Spain
[f] University of Idaho, Research and Extension Center, Kimberly, ID, 83341, USA

ARTICLE INFO

Keywords:
Basal crop coefficients
K_{cb} under full cover
Density coefficient
f_c from ground observations
f_c from NDVI
Estimates of K_{cb} for trees and annual crops
Operational K_{cb} from f_c with SIMS framework

ABSTRACT

The current study aims at reviewing and providing advances on methods for estimating and applying crop coefficients from observations of ground cover and vegetation height. The review first focuses on the relationships between single K_c and basal K_{cb} and various parameters including the fraction of ground covered by the canopy (f_c), the leaf area index (LAI), the fraction of ground shaded by the canopy (f_{shad}), the fraction of intercepted light (f_{light}) and intercepted photosynthetic active radiation (f_{IPAR}). These relationships were first studied in the 1970's, for annual crops, and later, in the last decennia, for tree and vine perennials. Research has now provided a variety of methods to observe and measure f_c and height (h) using both ground and remote sensing tools, which has favored the further development of K_c related functions. In the past, these relationships were not used predictively but to support the understanding of dynamics of K_c and K_{cb} in relation to the processes of evapotranspiration or transpiration, inclusive of the role of soil evaporation. Later, the approach proposed by Allen and Pereira (2009), the A&P approach, used f_c and height (h) or LAI data to define a crop density coefficient that was used to directly estimate K_c and K_{cb} values for a variety of annual and perennial crops in both research and practice. It is opportune to review the A&P method in the context of a variety of studies that have derived K_c and K_{cb} values from field measured data with simultaneously observed ground cover f_c and height. Applications used to test the approach include various tree and vine crops (olive, pear, and lemon orchards and vineyards), vegetable crops (pea, onion and tomato crops), field crops (barley, wheat, maize, sunflower, canola, cotton and soybean crops), as well as a grassland and a Bermudagrass pasture. Comparisons of K_{cb} values computed with the A &P method produced regression coefficients close to 1.0 and coefficients of determination $\geq$ 0.90, except for orchards. Results indicate that the A&P approach can produce estimates of potential $K_{cb,}$ using vegetation characteristics alone, within reasonable or acceptable error, and are useful for refining K_{cb} for conditions of plant spacing, size and density that differ from standard values. The comparisons provide parameters appropriate to applications for the tested crops. In addition, the A&P approach was applied with remotely sensed f_c data for a variety of crops in California using the Satellite Irrigation Management Support (SIMS) framework. Daily SIMS crop ET ($ET_{c\text{-}SIMS}$) produced K_{cb} values using the FAO56 and A&P approaches. Combination of satellite derived f_c and K_{cb} values with ET_o data from Spatial CIMIS (California Irrigation Management Information System) produced ET estimates that were compared with daily actual crop ET derived from energy balance calculations from micrometeorological instrumentation ($ET_{c\ EB}$).Results produced coefficients of regression of 1.05 for field crops and 1.08 for woody crops, and R^2 values of 0.81 and 0.91, respectively. These values suggest that daily $ET_{c\text{-}SIMS}$ -based ET can be accurately estimated within reasonable error and that the A&P approach is appropriate to support that estimation. It is likely that accuracy can be improved via progress in remote sensing determination of f_c. Tabulated K_{cb} results and calculation parameters are presented in a companion paper in this Special Issue.

* Corresponding author.
E-mail addresses: lspereira@isa.ulisboa.pt, luis.santospereira@gmail.com (L.S. Pereira).

https://doi.org/10.1016/j.agwat.2020.106197
Received 30 December 2019; Received in revised form 31 March 2020; Accepted 5 April 2020
0378-3774/ © 2020 Elsevier B.V. All rights reserved.

1. Introduction

Over many years, studies have aimed at deriving crop coefficients from assessments of the relationships between a single K_c or basal K_{cb} and a variety of vegetation parameters including the fraction of ground covered by the canopy (f_c), the leaf area index (LAI), the fraction of ground shaded by the canopy (f_{shad}), the fraction of intercepted light (f_{light}) and intercepted photosynthetic active radiation (f_{IPAR}). Other crop canopy characteristics such as crop height (h) or tree crop size have been considered. Applications include a relatively large number of field and tree crops beginning nearly 50 years ago while studies relative to vines and trees are more recent, only 20 years ago.

The relation of relative ET (K_c or K_{cb}) with amount of vegetation has an obvious and physical basis, where more plant leaf surface area means more total bulk stomatal surface and conductance and more opportunity for diffusion of water vapor from leaves as transpiration (Monteith, 1965, 1981). Similarly, more ground cover or leaf area by vegetation means more surface area for absorption of solar photons and subsequent conversion of that energy into ET. Therefore, given similar stomatal conductance and leaf and canopy architectural properties, one might expect to see, under adequate soil moisture conditions, the relative ET from a vegetated area to increase with increasing ground cover or leaf area (Monteith, 1981). Energy constraints create an upper limit on total relative ET with increasing leaf area beyond some limit, often regarded to be approximately LAI = 3 (Ritchie, 1972), with an asymptotic relationship between K_{cb} and LAI as LAI approaches or exceeds 3 and extending to about LAI = 6 (Tanner and Jury, 1976). The fraction of ground covered by the canopy, on the other hand, tends to have a more linear relationship with relative ET due to a more direct, proportional relationship between interception of solar photon flux by the canopy and its conversion to transpiration (Williams and Ayars, 2005; López-Urrea et al., 2014) as described in the following sections.

FAO56 (Allen et al., 1998) introduced a standardized approach to relate the basal K_c during the midseason period,$K_{cb\ mid}$, to LAI or f_c using a K_{cb} value representing K_{cb} under conditions of full cover, $K_{cb\ full}$, represented by LAI > 3. The proposed $K_{cb\ mid}$-LAI and $K_{cb\ mid}$-f_c equations were aimed at estimating $K_{cb\ mid}$ for natural, non-typical or non-pristine agricultural vegetation not included in the standardized tables, and were not directed toward applications for common agricultural crops. $K_{cb\ end}$ was estimated by scaling the $K_{cb\ mid}$ equations according to conditions at the end of the season and the length of the late season. A resistance correction factor (F_r) was proposed for the LAI- and f_c-based equations to take into consideration stomatal control by vegetation. In the FAO56 approach, estimates for $K_{cb\ full}$ were targeted toward non-pristine agricultural crops based on FAO56 tabulated $K_{cb\ mid}$ values for a considered crop after adjustment for climate relative to the standard sub-humid and calm conditions (RH_{min} = 45 % and u_2 = 2 m s^{-1}). A second estimate for $K_{cb\ full}$ was directed to natural vegetation, non-full cover crops or crops not listed in FAO56. It utilized the $K_{cb\ mid}$ for full cover vegetation (LAI > 3) and was estimated as a function of the mean maximum crop height ($K_{cb\ h}$ = 1 + 0.1 h) where $K_{cb\ h}$ was limited to 1.2, the proposed upper limit for K_{cb} for tall vegetation having full ground cover with LAI > 3. $K_{cb\ h}$ should also be adjusted for climate. The use of the $K_{cb\ mid}$-f_c equation was directed toward trees and shrubs. However, the use of $K_{cb\ full}$ estimated from $K_{cb\ h}$ reveals that it may be applicable to a wide range of conditions for agricultural crops, particularly to orchards and vineyards where large ranges in f_c and h exist and large ranges in $K_{cb\ mid}$ occur. Therefore, Allen and Pereira (2009) extended the application of the FAO56 equations through the development of a density coefficient (K_d) computed either from f_c and h or from LAI. That approach, referred herein as A&P approach, included specific equations for K_c and K_{cb} for orchards and vineyards that considered the amount of active ground cover. Their article included the tabulation of parameters for a variety of crops, as well as tabulated K_c and K_{cb} values for orchards and vineyards that considered a range of crop densities or age and the presence or absence of active ground cover.

This current study provides an important opportunity to review and revise related applications and concepts. The objectives of this article consist of: (a) reviewing and revising the use of K_c and K_{cb} relations with f_c, LAI and other indicators of canopy light and energy interception; (b) reviewing approaches relative to deriving f_c from field and remote sensing observations; (c) testing applications of the A&P approach to compute K_{cb} against model-derived K_{cb}; and (d) parameterization of A&P equations for field and tree crops. Tabulated values for K_{cb} estimated with the A&P equations are presented in a companion paper (Pereira et al., 2020c, this Special Issue).

Section 2 reviews studies on relationships between K_c or K_{cb} and LAI, f_c or other fractions of canopy light or radiation interception by field and vegetable crops, and tree and vine crops. The derivation of f_c from field observations and remote sensing are briefly dealt with in Section 3. An update of the A&P approach to compute K_c and K_{cb} is described in Section 4. The test of A&P equations for various field, vegetable, tree and vine crops is presented in Section 5, while Section 6 discusses the application of the A&P approach in the Satellite Irrigation Management Support framework to predict daily crop ET. Section 7 provides advice and recommendations for users.

2. Review of relationships between crop coefficients and the fraction of ground cover or leaf area index

2.1. Field and vegetable crops

Ritchie and Burnett (1971) introduced the use of the ratio E_p/E_o representing plant evaporation (E_p) to potential evaporation (E_o), which corresponds to the currently used K_{cb} or transpiration coefficient, and developed power relationships with LAI and f_c for both cotton and grain sorghum based upon two years of observations. In their pioneering work, data relative to both crops and both experimental years were fitted by the same curve. In a later pioneering study, Al-Khafaf et al. (1978) used two years of experiments with cotton and sorghum and found an exponential relationship between the E_p/E_o ratio and LAI. As with the study of Ritchie and Burnett (1971), all data were fitted to the same equation. In contrast, Tanner and Jury (1976) did not use an E_p/E_o ratio, but demonstrated that actual ET and T of a potato crop observed in a lysimeter were closely related to LAI. Al-Kaisi et al. (1989) obtained non-linear relationships between maize K_c and LAI using treatments that allowed detection of the role of soil evaporation, thus providing for a distinction between K_c and K_{cb} as later defined. Villalobos and Fereres (1990) fit an exponential curve to the K_{cb}-LAI data for three crops: corn, cotton, and sunflower.

Medeiros et al. (2001) reported a third degree polynomial relationship between K_{cb} and LAI for beans; however, in a later study (Medeiros et al., 2016) a quadratic equation was fitted to relate K_{cb} with LAI. Studies by Duchemin et al. (2006) using remote sensing have shown that the K_c-LAI relationship for wheat could fit a unique exponential curve over 13 fields and three years of observations, however with large dispersion along the fitted curve. Jiang et al. (2014) reported that K_c and K_{cb} could be related with LAI using exponential relationships for maize seeded at various densities that produced diverse LAI throughout the growing season. Common to the above referred studies are the non-linear relationships between LAI and K_c or K_{cb}. In contrast, Borges et al. (2015) used the Bowen ratio-energy balance (BREB) to derive K_{cb} for melon, and found a linear relation with LAI.

Ritchie and Burnett (1971) also studied the relationship between the ratio E_p/E_o and the fractional ground cover or f_c. Non-linear relationships were found, which were different for sorghum in two experimental years, since different row spacings were used. Later, Grattan et al. (1998) developed non-linear relationships between ground cover and crop coefficients for vegetable and row crops in California using the BREB method to determine crop ET. Crops studied included artichoke, pinto beans, broccoli, lettuce, melon, onion, and strawberry. Those

authors concluded that K_c changed as a quadratic function of the percentage ground cover or f_c, but linear fits were observed for data collected before midseason. Similarly, using weighing lysimeters, Bryla et al. (2010) found that quadratic equations could describe the relationships between K_{cb} and f_c for broccoli, lettuce, bell pepper and garlic. Graphical results of both studies, evaluated and reported in Allen and Pereira (2009), suggest that linear relationships may accurately describe K_{cb}–f_c relations before maximum vegetation development. Medeiros et al. (2001) reported third degree polynomials relating K_{cb} to f_c for beans.

Using remote sensing observations, Heilman et al. (1982) found a linear relationship between K_c and f_c for four alfalfa plots. Later, López-Urrea et al. (2009a) derived a linear equation relating onion K_{cb} and f_c, with data obtained with a weighing lysimeter. Similarly, López-Urrea et al. (2009b) reported a linear relationship between spring wheat K_c and f_c. López-Urrea et al. (2014) fit linear equations to K_{cb}-f_c relationships for sunflower using lysimeter data, however with different slopes of regression lines for each of two years of data. A linear relationship between K_c and f_c was reported by Zhang et al. (2015) for sugarcane during the crop development stage, with f_c obtained from NDVI. Lozano et al. (2016) reported a linear relationship between K_c and f_c for strawberries and López-Urrea et al. (2016) found good linear relationship between K_{cb} and f_c values for two years of biomass sorghum data observed in lysimeters. In addition, these authors reported an excellent agreement between Normalized Difference Vegetation Index (NDVI) and both K_{cb} and f_c. Finally, Trout and DeJonge (2018) reported a linear relationship between maize f_c and K_{cb} relative to alfalfa reference ET, for $f_c \leq 0.80$, and that linearity was not preserved beyond that threshold. Those authors assumed that this break in the linearity of K_{cb}-f_c was caused by maize tasseling.

The above review shows that relationships between K_c or K_{cb} and f_c are, in general, non-linear relative to the full crop season of field and vegetable crops, but may be linear during vegetation development. That non-linearity likely led to the adoption in FAO AquaCrop of a model-adjusted f_c, which is multiplied by $K_{cb\ max}$ to obtain actual K_{cb} and, therefore, to estimate actual transpiration (Raes et al., 2009; Steduto et al., 2009). However, this concept applies only for cases of full canopy cover for field and vegetable crops. In contrast, evidence for relationships between K_c and/or K_{cb} and LAI or f_c led Allen et al. (1998) to adopt in FAO56 predictive equations for K_c and K_{cb} from LAI and f_c, which were later improved upon by Allen and Pereira (2009).

2.2. Tree and vine crops

Studies on tree and vine crops were developed later than those for annual crops. The first study relating K_c with mid-day light intercepted by the canopy (f_{light}), which is a good estimator of f_c, was reported by Johnson et al. (2000) for mature peach trees, which was followed by Ayars et al. (2003). A linear relationship was found in these studies. Later, for Thompson seedless grapevine, Williams and Ayars (2005) also found a linear relationship between K_c and the fraction of area shaded (f_{shad}), again a good estimator of f_c. Goodwin et al. (2003, 2006) reported a strong linear relationship between K_{cb} and f_c and effective area of shade for peaches, where f_c was estimated using a combination of digital photographs of the tree taken from the direction of the sun and the fraction of PAR intercepted on the soil surface within the area of shade cast by the tree.

López-Urrea et al. (2012) reported good linear regressions relating K_{cb} and f_c observed in a weighing lysimeter for a “Tempranillo” vineyard over a three year period. The authors fit three equations to the three years, but a single equation could be adopted using all data, however with a smaller coefficient of determination. Later, Montoro et al. (2016) showed that fitted linear K_{cb} – f_c relationships were different for irrigated and non-irrigated conditions, which likely caused reduced $K_{cb\ act}$ when vines were not irrigated. Also for a “Tempranillo” vineyard, Picón-Toro et al. (2012) found linear relationships between K_{cb} and LAI, f_{IPAR} and f_c over a total of 5 years of data. Ferreira et al. (2012) studied five vineyards in different locations using eddy covariance and adopted linear relationships for the $K_{cb\ max}$-LAI and $K_{cb\ max}$-f_c relations. In contrast, Zhao et al. (2018) found a non-linear relationship between K_{cb} and LAI for a vineyard, with different curves for all the years of experimentation.

Following the tree K_c–f_{light} studies referenced above, research relative to tree crops has tested various indicators of canopy characteristics. Girona et al. (2011), for a five-year experiment with apple (cv ‘Golden Smoothee’) and pear (cv ‘Conference’), reported that K_c observed in large weighing lysimeters varied exponentially with f_{IPAR} observed at noon. Responses of both tree crops were however different: while all apple data fit the same curve well, regardless of the year, different equations were required to fit the pear data from different years, depending on the tree age. Those authors hypothesized that this different behavior may be related to differences in the canopy properties between the two tree crops, with pear canopies having higher porosity than apple canopies, thus higher light penetration, while apple canopies were denser and taller. In addition, the authors concluded that midday light interception did not adequately account for differences in K_c across both species. Auzmendi et al. (2011) reported that the relationships between actual transpiration ($T_{c\ act}$) and f_{IPAR} for apples were linear and observed that pre-harvest and post-harvest data behaved differently, likely because the latter consisted of smaller $T_{c\ act}$ and f_{IPAR} values. Marsal et al. (2013) developed different canopy characteristics for apple trees based on plant height (h) and width (w): the ratio h/w designated slenderness, and the difference LAI – h/w, called leaf overlapping. They used these indicators to characterize the canopy porosity of apple trees and to model $K_{c\ mid}$ variability. A different canopy indicator was used by González-Talice et al. (2012), who reported linear relationships between tree cross-sectional area (TCSA) and K_{cb}; TCSA was used as an indicator of ground cover shaded area. Moreover, these authors found that linear regressions for TCSA-K_{cb} were similar for Galaxy and Fuji varieties but both differed from the equation used to fit Granny Smith data.

Relationships between K_c-f_c for trees and vines were developed only relatively recently. For pecans, and using remote sensing data over a number of cropped fields in New Mexico, Samani et al. (2011) found a linear relationship between the ratio $K_c/K_{c\ ref}$ and f_c, where $K_{c\ ref}$ was the K_c measured for a mature pecan orchard with $f_c = 80$ %. That linear relationship proved acceptable for a pecan orchard in South Africa (Ibraimo et al., 2016) but those authors concluded that pecans did not show a linear relationship between K_c and midday f_{IPAR} and it was not possible to use the relationship proposed by Samani et al. (2011) predictively. Espadafor et al. (2015) used four years of lysimeter observations in a young almond tree orchard, where f_c increased from 3 to 48 %, to assess the time evolution of the ratios K_{cb}/f_{IPAR} and K_{cb}/f_c over the last two years. They found nearly constant ratios through time but no curve fittings were performed. Lately, López-López et al. (2018) assessed the behavior of the ratio K_{cb}/f_c for almonds but did not fit any equation to the relationships between variables; however, values for that ratio differed when computed from lysimeter or from field water balance.

The above review shows that relationships between K_c or K_{cb} and f_c or LAI for trees and vine crops, contrary to field and vegetable crops, are only recently studied, and that different indicators of canopy interception of radiation have been used. Generally, predictive K_c and K_{cb} equations proposed in FAO56 using f_c or LAI data were assumed to be applicable to trees and vines. Allen and Pereira (2009) developed predictive equations for K_c and K_{cb} from LAI and f_c, focusing on trees and vines, as analyzed further in this article.

2.3. Crop coefficients from ground cover and height

The FAO56 $K_{cb\ mid}$-LAI and $K_{cb\ mid}$-f_c relationships described above may be used predictively after estimating $K_{cb\ full}$, adjusting for climate

conditions and considering the use of the resistance correction factor, F_r, when the crop exhibits more stomatal control than standard agricultural crops. Conversely, the simple FAO56 relations of K_c or K_{cb} with f_c, LAI, f_{shad} or f_{IPAR} were generally not developed to be used predictively, but rather mainly to discuss the behavior and suitability of derived K_c and K_{cb} values. To expand the predictability of those FAO56 equations, Allen and Pereira (2009) developed the A&P approach as a refinement and upgrade of the referred FAO56 equations. A coefficient of density (K_d) from either LAI or f_c and h was defined to promote standardization and visual reproducibility. Parameter values were proposed and new K_c and K_{cb} values for various crops and crop densities, mainly for tree and vine crops, were considered. Tabulated K_c and K_{cb} values using the A&P approach for various crops, primarily for trees and vines having diverse crop densities and heights, were later provided by Jensen and Allen (2016). More recently, Johnson and Melton (2017) revised the application of the A&P approach and proposed updated parameters for a wide panoply of field, vegetable and fruit woody crops of California. The approach is gaining usage by many researchers, however often with limited information regarding the applications.

Numerous A&P applications have used the dual K_c water balance model SIMDualKc because the approach is incorporated into the model (Rosa et al., 2012a, b) and is used to adjust K_{cb} values according to observed or simulated f_c and h values. Examples include field research applications to tree and vine crops including peach (Paço et al., 2012), olives (Paço et al., 2014, 2019), vineyards (Fandiño et al., 2012; Cancela et al., 2015), as well as to field crops including soybeans (Wei et al., 2015) and bermudagrass (Paredes et al., 2018). Miao et al. (2016) used the A&P approach to develop a procedure to compute K_{cb} for relay intercrops, and Rosa et al. (2016) developed a ET-K_{cb} computational application for saline conditions. Related results from these applications are analyzed in Section 5.

Other A&P applications included estimation and analysis of K_{cb} for olives (Conceição et al., 2017; Puppo et al., 2019), citrus (Taylor et al., 2015) and maize (Ding et al., 2013). Qiu et al. (2013) and Zheng et al. (2013) applied the A&P approach to estimate the K_c of tomato cropped in both a greenhouse and open field. Pôças et al. (2015) used the A&P approach to validate computations of K_{cb} for maize, barley and olives using remote sensing (RS) vegetation indices: NDVI and SAVI (soil-adjusted vegetation index), and Santos et al. (2012) used that approach to parameterize the RS model METRIC (mapping evapotranspiration at high resolution with internalized calibration). All applications produced relatively good accuracy for estimates of K_{cb} values.

3. Determining the fraction of ground cover

The observation of f_c involves some complexity, however, depending upon the desired accuracy. Adams et al. (1976) described an early description of a method for field determination of the fraction of ground cover, or the fraction of ground shaded by the canopy in row crops as it is referred to in their study. It refers to the use of a meter-stick on the soil surface adjacent to plants and parallel to the row. Later, Adams and Arkin (1977) compared various methods to determine ground cover and concluded that the meter-stick method is as accurate, faster, simpler, and more economical than the other methods used. They reported that there were no significant differences in measurement results using the meter-stick method, overhead photographs, spatial quantum sensor, or traversing quantum cell. Cihlar et al. (1987) developed a methodology for estimating green plant cover based on a supervised classification technique of digital photographic images using a maximum probability algorithm, with the purpose of assigning the current classes of green vegetation in the image.

The use of overhead photographs has continued, with improved equipment and varied sophistications in separating canopy cover from background. Goodwin et al. (2006) reported the estimation of f_c using a combination of digital photographs of the tree taken from the direction of the sun and the fraction of PAR intercepted on the soil surface within the area of shade cast by the tree. Er-Raki et al. (2007) reported on the use a hemispherical canopy photo apparatus equipped with a fisheye lens to take photos above a wheat canopy, Hunsaker et al. (2013) reported on the use of a digital camera mounted on a hand-held aluminum pole to allow nadir views, and Trout and DeJonge (2018) reported the use of a digital camera from a nadir view 6 m above the ground surface. The main advances have come from the differentiation of digital image pixels relative to the plant canopy and background (soil, surface residue, and senesced leaves) particularly when digital images are used. A different approach was used by Martinez-Cob et al. (2014) who reported on the use of pyranometers for estimation of f_c at remote sites while adopting photographical techniques for *in-situ* observation. The main issues consist of taking the images near noon under a near-nadir condition. However, the use of digital images of trees to obtain various canopy features has different requirements as described by Espadafor et al. (2015).

Duan et al. (2017) compared f_c estimates from experimental plots cropped with cotton, sorghum and sugarcane with images and ortho-mosaics captured by a low altitude UAV. The authors reported good agreement between ground cover estimates from ortho-mosaic and images when the target was positioned at a near-nadir view at the centre of the image. The use of a digital camera from directly overhead of the canopy and image analysis to calculate the ratio of green leaf pixel to the whole photograph was also reported by Fan et al. (2017). Also recently reported was the precise detection of f_c for a lettuce crop using digital photography, which allows measurement of the diameter of the plants with help of appropriate software, namely relative to color selection (Fernández-Pacheco et al., 2014; Hernández-Hernández et al., 2016, 2017). A web application was developed by González-Esquiva et al. (2017). An application to diverse crops is reported by Zhang et al. (2018), who used nine color vegetation indices calculated from time series of digital photographs to develop an f_c estimation model applicable to sugarcane, maize, cotton and paddy rice.

Currently, f_c is commonly obtained from remote sensing. Trout et al. (2008) produced diverse advances in remote sensing of f_c, namely using NDVI from Landsat 5, after establishing a linear relationship between NDVI and f_c for a variety of crops. Later, among others, López-Urrea et al. (2009b, 2016); Johnson and Trout (2012); Campos et al. (2014); Pôças et al. (2015); Zhang et al. (2015) and de la Casa et al. (2018) reported on the relationships between f_c and various vegetation indices, mainly NDVI and SAVI. Imukova et al. (2015) used high-resolution RapidEye satellite images to determine the spatial and temporal dynamics of the green vegetation fraction of croplands.

4. Predicting K_{cb} from fraction of ground cover and height using a density coefficient

4.1. Background concepts

The two-step crop coefficient-reference ET method, K_c x ET_o, has been a successful and dependable means to estimate crop evapotranspiration (ET_c) and crop water requirements since the early 1970's (Doorenbos and Pruitt, 1977; Allen et al., 1998). The method uses weather data to estimate the grass reference ET_o and multiplies it by a crop coefficient (K_c) that represents the relative rate of evapotranspiration from a specific crop and condition to that of the reference crop (ET_c/ET_o). The reference condition is ET from a clipped, cool season, well-watered grass (ET_o) and represents a near maximum rate of ET that varies with weather conditions. The calculation of ET_o has been standardized by FAO (Allen et al., 1998, 2006) followed by the American Society of Civil Engineers (ASCE-EWRI, 2005; Jensen and Allen, 2016).

The K_c-ET_o approach provides a simple, convenient and reproducible way to estimate ET from a variety of crops and climatic conditions (Allen et al., 1998; Pereira et al., 1999, 2015). Crop

coefficient curves have been developed and were reported for a wide range of agricultural crops in FAO56 (Allen et al., 1998, 2007) and their standardized values are currently updated for vegetable and field crops (Pereira et al., 2020a, b, this Special Issue). The standardized K_c is regarded as generally transferable among regions and climates under the assumption that the ET_o accounts for nearly all variation caused by weather and climate and the K_c represents the relative fraction of ET_o that is governed by amount, type and condition of vegetation when cropped under standard, pristine conditions. Under most conditions, K_c values can be quite accurately estimated through their relations with the fraction of ground covered or shaded by vegetation, as discussed in previous sections, the height of the vegetation and the amount of stomatal regulation under moist soil conditions as proposed by Allen et al. (1998) and detailed in the Allen and Pereira (2009), A&P approach.

The value for K_c for conditions of water and/or salinity stress is generally determined by reducing the K_c estimate via a stress coefficient K_s using a daily soil water balance (SWB) model, e.g., the SIMDualKc model (Rosa et al., 2012a, b), and partitioning the K_c into transpiration and evaporation components. Adopting the dual K_c approach, K_c is defined as:

$$K_c = K_s K_{cb} + K_e \quad (1)$$

where K_{cb} is the basal crop coefficient representing the ratio between crop transpiration and ET_o, K_e is the soil evaporation coefficient representing the ratio between soil evaporation and ET_o, and K_s is a dimensionless 'stress' coefficient whose value is dependent on available soil water and soil and crop salinity related characteristics (Allen et al., 1998; Minhas et al., 2020). The value for K_s is 1 unless available soil water and/or salinity limits transpiration, in which case $K_s < 1$. Estimation of K_e for bare soil conditions is described in Allen et al. (1998, 2005b) and Allen (2011).

Fig. 1 shows the FAO segmented approach to describe the K_c curves, where the continuous seasonal curve is broken into four linear segments representing the initial, development, midseason and late season periods (Doorenbos and Pruitt, 1977; Allen et al., 1998, 2005a). The advantage of the FAO K_c curve is that only three key values for K_c need to be determined: $K_{c\ ini}$ during the initial period, $K_{c\ mid}$ during the mid-season period, and $K_{c\ end}$ at the end if the late season period. The FAO procedure for standard K_c values refers to mean standardized daily minimum relative humidity $RH_{min} = 45$ % and mean wind speed at 2 m, $u_2 = 2\ m\ s^{-1}$. For climates with RH_{min} and u_2 differing from those values, the standardized K_c values tabulated in FAO-56, or updated in Pereira et al. (2020a, b, this Special Issue), are adjusted for all $K_{c\ mid}$ and $K_{cb\ mid}$, as well as for $K_{c\ end}$ and $K_{cb\ end}$ larger than 0.45, as:

$$K_{c\,mid/end} = K_{c\,mid/end\,(Table)} + [0.04\,(u_2 - 2) - 0.004\,(RH_{min} - 45)]\left(\frac{h}{3}\right)^{0.3} \quad (2)$$

where $K_{c\ mid/end\ (Table)}$ is the value for $K_{c\ mid}$, $K_{cb\ mid}$, $K_{c\ end}$ or $K_{cb\ end}$ for the above referred standard climate, and h is the mean maximum plant height (m) during the midseason period, or full cover period. Eq. (2) is valid for h up to 20 m (Allen et al., 1998, 2005a). When the crop dries in field ($K_{c\ end} \leq 0.45$) the adjustment by Eq. (2) is not required. The values for RH_{min}, u_2 and h need only to be approximate values averaged over the mid-season and late-season periods. Eq. (2) helps to account for increases in maximum expected ET rates limited by environmental energy relative to the grass-based reference ET_o. The increases are strongest for tall vegetation that can have greater aerodynamic roughness and leaf area as compared to the clipped grass reference.

4.2. Estimating K_c curves from fraction of ground cover

For expanses of vegetation large enough that an equilibrium boundary is established so that general one-dimensional equations such as the Penman-Monteith apply, a maximum upper limit on ET is established due to the law of conservation of energy. Therefore, for large expanses of vegetation (larger than about 500 to 2000 m^2), the K_c development process has upper limits for K_c of 1.2–1.3 for the grass reference. However, as discussed by Allen et al. (2011) and Pereira et al. (2020a, b, this Special Issue), under conditions of "clothesline effects" (where vegetation height exceeds that of the surroundings) or "oasis effects" (where vegetation has higher soil water availability than the surroundings) peak K_c may exceed those limits. Caution is required when extrapolating ET measurements from small vegetation plots to large stands or regions because overestimation of ET may occur.

An upper, energy-constrained limit on K_c, termed $K_{c\ max}$, is defined as the maximum value for K_c following rain or irrigation and is governed by the amount of energy available for evaporation of water. The $K_{c\ max}$ varies with general climate, ranging from about 1.05–1.30 (Allen et al., 1998, 2005a):

$$K_{c\,max} = \max\left(\left\{1.2 + [0.04\,(u_2 - 2) - 0.004\,(RH_{min} - 45)]\left(\frac{h}{3}\right)^{0.3}\right\}, \{K_{cb\,(Table)} + 0.05\}\right) \quad (3)$$

where u_2, and RH_{min} are averaged daily u_2 and RH_{min} values during the growth period, $K_{cb\ (Table)}$ is the value for K_{cb} for the standardized climate, and h is the mean plant height (m) during the period of calculation (initial, development, midseason, or late-season).

Following the A&P approach, the basal K_{cb}, because it represents mostly transpiration, depends upon the amount of vegetation and can be expressed as a function of a density coefficient, K_d, as:

$$K_{cb} = K_{c\,min} + K_d(K_{cb\,full} - K_{c\,min}) \quad (4)$$

where K_{cb} is the approximation for K_{cb} for vegetation structure and extent represented by the density coefficient, K_d, defined hereafter; $K_{cb\ full}$is the estimated basal K_c at peak plant growth under conditions having nearly full ground cover (or LAI > 3); and $K_{c\ min}$ is the minimum basal K_c for bare soil (0.15 under typical agricultural conditions where some subsurface soil moisture exists). For tree crops having grass or other ground cover, Eq. (4) takes a different form that considers transpiration by the active ground cover, thus:

$$K_{cb} = K_{cb\,cover} + K_d\left(\max\left[K_{cb\,full} - K_{cb\,cover}, \frac{K_{cb\,full} - K_{cb\,cover}}{2}\right]\right) \quad (5)$$

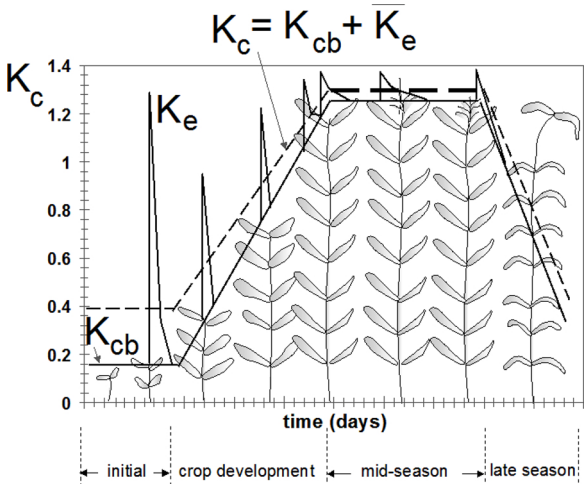

Fig. 1. Representative FAO crop coefficient curve and four growing stages (after Allen et al., 1998). The solid line shows the basal crop coefficient, the solid peaks shows the soil evaporation coefficient, and the dashed line shows the single time averaged crop coefficient.

where $K_{cb\ cover}$ is the K_{cb} of the active ground cover in the absence of tree foliage. The second term of the max function reduces the estimate for $K_{cb\ mid}$ by half the difference $K_{cb\ full} - K_{c\ cover}$ when this difference is negative. This accounts for impacts of shading by vegetation when $K_{cb} < K_{cb\ cover}$ due to larger stomatal conductance of the ground-cover. Eq. (5) applies to estimate K_{cb} during any period. As described by Allen and Pereira (2009), the approach of Eq. (5) can be similarly applied to estimate a single K_c coefficient.

$K_{cb\ full}$ can be approximated as a function of mean plant height and adjusted for climate following Allen et al. (1998):

$$K_{cb\,full} = F_r\left(\min(1.0 + k_h\,h,\ 1.20) + [0.04(u_2 - 2) - 0.004(RH_{min} - 45)]\left(\frac{h}{3}\right)^{0.3}\right) \quad (6)$$

where h, u_2 and RH_{min} were defined previously but herein referring to the mid-season. The value for $K_{cb\ full}$ represents a general upper limit on $K_{cb\ mid}$ for vegetation having full ground cover and LAI > 3 under full water supply. Eq. (6) suggests that an upper bound for $K_{cb\ full}$ is 1.20 plus adjustment for nonstandard climate. Effects of crop height are considered through the sum $1 + k_h\,h$, with $k_h = 0.1$ for tree and vine crops as well as tall field crops, and $k_h = 0.2$ for short crops and vegetables as described in following sections. Eq. (6) produces increases in $K_{cb\ full}$ with plant height and more arid climate. The parameter F_r applies a downward adjustment ($F_r \leq 1.0$) if the vegetation exhibits more stomatal control on transpiration than is typical of most annual agricultural crops. Examples are provided in the following sections. Adopting the Allen et al. (1998) calculation procedure for F_r, it is assumed:

$$F_r \approx \frac{\Delta + \gamma\,(1 + 0.34\,u_2)}{\Delta + \gamma\left(1 + 0.34\,u_2\frac{r_l}{100}\right)} \quad (7)$$

where r_l is mean leaf resistance for the vegetation in question [s m^{-1}], Δ is the slope of the saturation vapor pressure vs. air temperature curve [kPa $^oC^{-1}$], and γ is the psychrometric constant [kPa $^oC^{-1}$], both relative to the period when $K_{cb\ full}$ is computed. This factor, F_r, is multiplied against the estimate for $K_{cb\ full}$ in Eq. (6) to adjust its value, which is particularly important in the case of perennials and the late season. The standard value for F_r is 1.0 because for most annual agricultural crops r_l is often approximately 100 s m^{-1}. Values for r_l for many agricultural and non-agricultural plants can be found in Allen et al. (1996) and Pereira and Alves (2013). The value for r_l is limited to $\geq$ 100 s m^{-1}.

The density coefficient K_d used in Eq. (4) describes the increase in K_{cb} with increase in amount of vegetation. As proposed by Allen and Pereira (2009), where LAI can be observed or estimated, K_d can be approximated under normal conditions as:

$$K_d = (1 - e^{[-0.7\,LAI]}) \quad (8)$$

where LAI is defined as the area of leaves per area of ground surface averaged over a large area ($m^2\,m^{-2}$) with consideration of only one side of 'green,' healthy leaves active in vapor transfer.

Where estimates of the fraction of ground surface covered by vegetation, f_c, are available, the K_d is estimated as:

$$K_d = \min\left(1,\ M_L\,f_{c\,eff},\ f_{c\,eff}^{\left(\frac{1}{1+h}\right)}\right) \quad (9)$$

where $f_{c\ eff}$ is the effective fraction of ground covered or shaded by vegetation [0.01–1] near solar noon, M_L is a multiplier on $f_{c\ eff}$ describing the effect of canopy density on shading and on maximum relative ET per fraction of ground shaded [1.0–2.0], and h is the mean height of the vegetation (m). $f_{c\ eff}$ is often observed as the shaded area near noon, between 11.00 and 15.00 as reported in Section 3. Estimation of $f_{c\ eff}$ for row crops was described by Allen et al. (1998). An estimation for trees was provided by Allen and Pereira (2009). $f_{c\ eff}$ is often determined from visual inspection.

The M_L multiplier on $f_{c\ eff}$ in Eq. (9) imposes an upper limit on the relative magnitude of transpiration per unit of ground area as represented by $f_{c\ eff}$ (Allen et al., 1998) and is expected to mostly range from 1.5 to 2.0, depending on the canopy density and thickness. M_L is an attempt to simulate the upper physical limits on transpiration imposed by water flux through the plant root, stem and leaf systems. M_L may have a low value when the canopy porosity is high. The value for M_L can be modified to fit the specific vegetation and experimental data.

5. Validation of K_{cb} prediction from fraction of ground cover and height using ground observations

The objective of this section is to demonstrate the application and ability of the A&P approach to reproduce standard and measured K_{cb} for a variety of trees and vines and vegetable and field crops. The standard K_{cb} used herein were derived from actual crop evapotranspiration data obtained through soil water balance procedures, based upon accurate soil moisture measurements, as well as by sap-flow and eddy covariance measurements whose data were ingested into the SIMDualKc model (Rosa et al., 2012a). The linearly-segmented K_{cb} curves were then computed through the calibration and validation of the model (Rosa et al., 2012b) using the observed soil water content, or the observed transpiration with sap-flow devices, or the crop ET measured with eddy covariance instrumentation. The K_{cb} values obtained through the calibration procedures are referred hereafter as $K_{cb\ SIMDualKc}$. K_{cb} values reported here were also obtained from crop ET accurately measured with large size weighing lysimeters located in the middle of large fields cultivated with the same crop and techniques used in the lysimeters (López-Urrea et al., 2016). These K_{cb} values are named herein as $K_{cb\ lysimeter}$. ET measurements and the K_{cb} derivation procedures are described in the publications cited for each crop. Parameters in the A&P functions were determined using a simplified trial and error procedure such that $K_{cb\ A\&P}$ approximate the $K_{cb\ SIMDualKc}$ or $K_{cb\ lysimeter}$ during various stages for each crop. Only the case study of Section 5.6 fit A&P parameters directly to experimental data. Ranges of values found for parameters give indication of values for parameters to be expected in practice. These ranges, in the case of trees and vines, refer to variation in f_c and h following pruning and natural plant growth during a stage; in the case of vegetable and field crops, refer to crop growth during a stage and, later, to senescence; and for grasses and pasture, refer to cuttings and regrowth.

Table 1
Ranges in parameters for the A&P approach used in Eqs. (4), (6), (7) and (9) to produce $K_{cb\ A\&P}$ values for olives.

Crop stages	h (m)[a]	$f_{c\ eff}$[a]	F_r	$K_{cb\ full}$	K_d	$K_{cb\ A\&P}$
Non-growing	3.0–4.0	0.18–0.34	0.55	0.61–0.64	0.26–0.51	0.17–0.33
Initial	3.0–3.6	0.27–0.34	0.55	0.61–0.64	0.40–0.51	0.21–0.33
Development	3.0–3.6	0.27–0.39	0.55–0.65	0.64–0.79	0.40–0.57	0.21–0.45
Mid-season	3.6–4.0	0.32–0.39	0.65	0.79–0.83	0.48–0.57	0.45–0.52
Late-season	3.6–4.0	0.35–0.39	0.65–0.55	0.63–0.83	0.48–0.59	0.40–0.52

[a] Field data from Paço et al. (2019).

5.1. Trees and vines

5.1.1. Olive

Data were provided from field research reported by Paço et al. (2019), which was performed during 2011–2013 in a 78 ha super-intensive olive orchard, located at Viana do Alentejo, southern Portugal. f_c values used with the A&P approach were obtained through field observations or using remote sensing (Pôças et al., 2015). $K_{cb\ SIMDualKc}$ values were derived from the calibration and validation of the SIMDualKc model using sap-flow transpiration measurements. Further validation was performed using eddy covariance measurements of $ET_{c\ act}$.

A value of $M_L = 1.5$ was used in Eq. (9) and $K_{cb\ full}$ was computed with Eq. (6) using $k_h = 0.1$. Table 1 provides the ranges of values for the terms of the A&P approach computed using observed data. Ranges are related with f_c changes due to pruning and related responses of trees, exacerbated by heavy pruning following exceptional frosts. F_r values were estimated after those tabulated by Allen and Pereira (2009). Fig. 2 shows the $K_{cb\ A\&P}$ estimated values compared with the $K_{cb\ SIMDualKc}$ values resulting from field observations during three growing seasons. The regression forced through the origin (FTO) produced a regression slope of $b_0 = 1.00$ (Fig. 3), thus there were no over or under-estimation trends.

5.1.2. Peach

In a study performed during 1998 and 1999 seasons in a commercial orchard located at Atalaia, Montijo, southern Portugal, Paço et al. (2012) measured peach transpiration using sap-flow ($T_{c\ act}$) along with ET measurements of eddy covariance (ET_{EC}). One year of $T_{c\ act}$ measurements was used to calibrate the SIMDualKc model and the other was used for model validation along with the ET_{EC} measurements. In this study, only one value for $f_{c\ eff} = 0.30$ was measured during the mid-season. Considering $M_L = 1.4$, $k_h = 0.1$ and $F_r = 1$, the calculated K_d was 0.41 when $K_{cb\ full}$ was 1.17, thus resulting in $K_{cb\ A\&P} = 0.51$, which compared well with the field derived $K_{cb\ SIMDualKc} = 0.50$.

5.1.3. Pear

A study was performed during two seasons, 2013 and 2014, in a 50 ha commercial 'Rocha' pear orchard located in Torres Vedras, western Portugal (Rosa, 2019). Spatially distributed soil water measurements were accurately performed with FDR devices. Other measurements included the water table depth. $f_{c\ eff}$ values were obtained from intercepted photosynthetically active radiation (f_{IPAR}) measured with AccuPAR LP-80 (Decagon Devices, USA). All measurements were used to calibrate and validate the SIMDualKc model and, therefore, to derive the $K_{cb\ SIMDualKc}$ (Fig. 4).

In the A&P approach, $M_L = 1.5$ was used and $K_{cb\ full}$ was computed with Eq. (6) using $k_h = 0.1$. Table 2 provides ranges for terms of the A&P approach computed using observed $f_{c\ eff}$ and h. F_r values were estimated following Allen and Pereira (2009). The FTO regression (Fig. 4) produced $b_0 = 0.98$, indicating a slight under-estimation tendency by the $K_{cb\ A\&P}$.

5.1.4. Lemon

A study was performed on lemons during two growing seasons, 2013 and 2014, in a 5 ha fully established lemon orchard (Rosa, 2019) located in Mafra, near the west coast of Portugal. As per the study on pear, soil water content was performed with FDR instrumentation at representative locations within the orchard. $f_{c\ eff}$ was obtained from f_{IPAR} measurements. The soil moisture-based ET data were used to calibrate and validate the SIMDualKc model and, therefore, to derive K_{cb} (Fig. 5).

In the A&P approach, $M_L = 1.2$ was used and $K_{cb\ full}$ was computed with Eq. (6) using $k_h = 0.1$. Table 3 provides ranges for the terms in the A&P approach computed using observed $f_{c\ eff}$ and h. F_r values were estimated after those tabulated by Allen and Pereira (2009). The FTO regression (Fig. 5) produced $b_0 = 1.03$, thus a slight over-estimation tendency for the $K_{cb\ A\&P}$.

5.1.5. Wine grapes

5.1.5.1. Vineyards with bare soil. Data were collected during two seasons for mature Tempranillo wine grapes and reported by López-Urrea et al. (2012). The water use of two grapevines was measured with a monolithic large weighing lysimeter installed in the center of a 1-ha plot, surrounded by a drip-irrigated vineyard of about 5 ha. ET_c values were calculated as the difference between lysimeter mass losses (from evaporation and/or transpiration) divided by the lysimeter area (9.0 m^2). The lysimeter container is 3 m × 3 m square and 1.7 m deep. The lysimeter soil-containing tank sits on a system of beams and a counterbalances that offsets the dead weight of the soil and the tank and reduces the load on the weigh beam by 1,000:1. The lysimeter mass resolution was 0.01 mm, and its accuracy was greater than 0.03 mm equivalent water depth. Two vines were planted in the lysimeter, each one occupying 4.5 m^2, i.e., the same as the vines outside the lysimeter, thus allowing for representative measurements of vineyard ET_c. Efforts were made to keep the vines inside the lysimeter growing at the same rate as the crop outside to minimize edge effects. The basal crop coefficient (K_{cb}) was obtained from the lysimeter K_c values minus the calculated K_e values using the FAO56 methodology (Allen et al., 1998). Additional information about the lysimeter facility and the technical features of the lysimeter may be found in López-Urrea et al. (2012).

In the A&P approach, M_L varied among the different stages, with M_L values of 1.1, 1.3 and 1.8 used, respectively for the initial, development and mid-season. $K_{cb\ full}$ was computed with Eq. (6) using $k_h = 0.1$. Table 4 provides for the terms of the A&P approach computed using f_c and h observations. F_r values were estimated after those tabulated by Allen and Pereira (2009). The regression forced through the origin (Fig. 6) produced $b_0 = 0.99$, thus, no under or over-estimation tendency for the $K_{cb\ A\&P}$ values.

5.1.5.2. Vineyards with active ground cover. Three examples are provided in this section; first an Albariño vineyard with permanent active ground cover at Pontevedra, Spain, and then two vineyards with the cv Godello and Mencía, at Valdeorras and Ribeira Sacra, respectively, Galicia, Spain, having active ground cover which transformed into mulch during the growing season. Two different trellis systems were utilized in the three examples. In all cases, $ET_{c\ act}$ was determined with a SWB and the soil water content was monitored with TDR. These data were used to calibrate and validate the SIMDualKc model, thus, to derive K_{cb} for the three vineyards.

The first example includes data for f_c and h data for mature Albariño wine grapes (semi-trellis system), which were reported by Fandiño et al. (2012). f_c and h values were measured during five growing seasons,

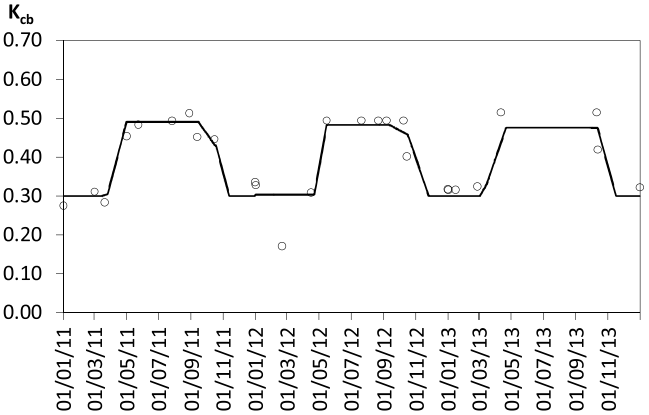

Fig. 2. Olive $K_{cb\ A\&P}$ estimates (○) compared with the $K_{cb\ SIMDualKc}$ curve (—) for the period 2011 to 2013 (Field data from Paço et al., 2019).

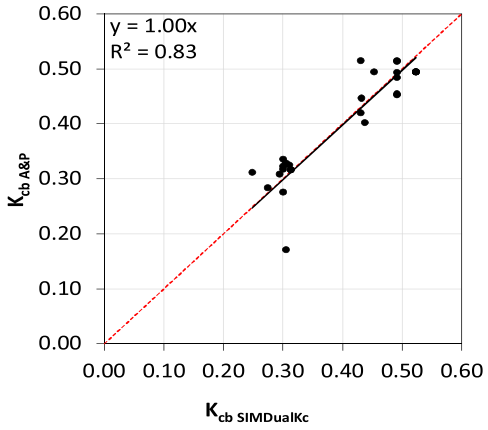

Fig. 3. Linear regression forced through the origin comparing $K_{cb\ A\&P}$ values with $K_{cb\ SIMDualKc}$ for olives; also depicted is the 1:1 line (- - -) (Field data from Paço et al., 2019).

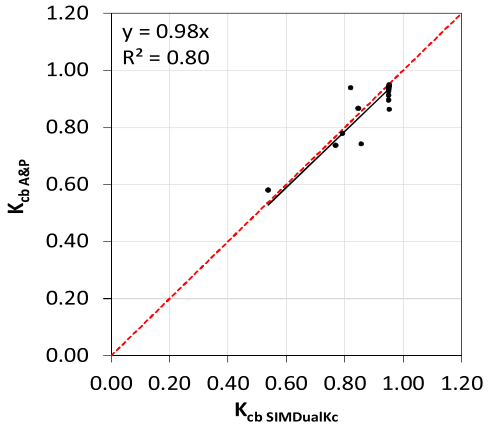

Fig. 4. Linear regression forced through the origin comparing $K_{cb\ A\&P}$ values with $K_{cb\ SIMDualKc}$ for 'Rocha' pears; also depicted is the 1:1 line (- - -) (Field data from Rosa, 2019).

Table 2
Ranges in parameters for the A&P approach used in Eqs. (4), (6), (7) and (9) to produce $K_{cb\ A\&P}$ values for 'Rocha' pears.

Crop stages	h (m)[a]	$f_{c\ eff}$[a]	F_r	$K_{cb\ full}$	K_d	$K_{cb\ A\&P}$
Development	3.4–3.7	0.45–0.57	0.95	1.03–1.05	0.68–0.86	0.58–0.91
Mid-season	3.5–3.7	0.57–0.62	0.95	1.05	0.86–0.90	0.91–0.95

[a] Field data from Rosa (2019).

with unpublished data from 2011 and 2012 seasons. An active ground cover was maintained in the inter-row area consisting of natural herbaceous vegetation. For active ground cover characterization, observations were performed during the crop season, including its density, height (h_{cover}) and fraction of green active ground cover ($f_{c\ cover}$). These characteristics changed throughout the season due to various cultivation practices, mainly mowing and application of herbicides along the vine row. An adjustment to the measured f_c was applied to determine $f_{c\ eff}$ (effective fraction of ground covered or shaded by vegetation) using the equations proposed by Rosa et al. (2012a). A complete description of observations, measurements, the SWB approach and the derivation of $K_{cb\ SIMDualKc}$ is provided by Fandiño et al. (2012).

In the A&P approach, $M_L = 1.5$ was used, $K_{cb\ full}$ was computed with Eq. (6), and $K_{cb\ A\&P}$ was determined using Eq. (5) due to the presence of an active ground cover in the inter-row during the entire season. $K_{cb\ gcover}$ (relative to the active ground cover vegetation) was determined with the SIMDualKc model taking into account different soil

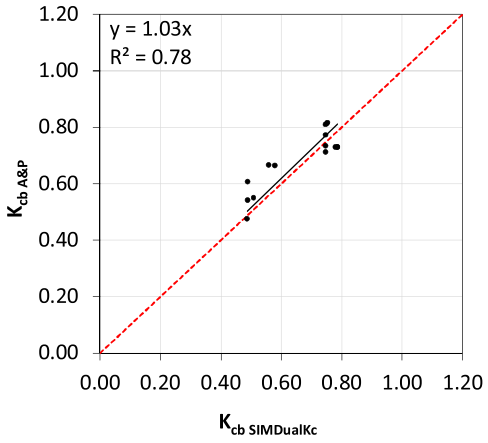

Fig. 5. Linear regression forced through the origin comparing $K_{cb\ A\&P}$ values with $K_{cb\ SIMDualKc}$ for lemon trees; also depicted is the 1:1 line (- - -) (Field data from Rosa, 2019).

management operations practiced during the season, which are reported in Fandiño et al. (2012). Table 5 presents ranges for the terms of the A&P approach computed using observations for f_c and h. F_r values for initial and midseason periods and for the end-season were taken from Fandiño et al. (2012), which were related to $K_{cb\ full}$ adjusted to local conditions. Fig. 7 shows the comparison of estimated $K_{cb\ A\&P}$ values with $K_{cb\ SIMDualKc}$ through a FTO regression, where $K_{cb\ SIMDualKc}$ values were derived from observations. Estimated values for the initial and development stages showed worse results during the five seasons, likely because the effects of the active ground cover were more important during these stages. The FTO regression (Fig. 7) produced $b_0 = 1.00$, thus no tendency for under- or over-estimation of the $K_{cb\ A\&P}$ values. The resulting error in daily K_{cb} estimation had an RMSE of 0.05.

The second group of vineyards represent data for f_c and h for mature Godello and Mencía wine grapes (vertical trellis on a double and single cordon system, respectively) that were reported by Cancela et al. (2015). Data from 2012 and 2013 were used in both cases, with f_c and h values measured during two growing seasons. A similar process to the Albariño vineyard was applied to produce the $K_{cb\ A\&P}$ values. $K_{cb\ gcover}$ was also determined using the SIMDualKc model taking into account variation in active ground cover during the season, with the ground cover mulched during the development stage. Table 6 presents ranges for the terms of the A&P approach computed using observations. F_r values for initial and midseason periods and for end-season were taken from Cancela et al. (2015) and related with $K_{cb\ full}$ adjusted to local conditions. Fig. 8 shows the comparison of estimated $K_{cb\ A\&P}$ values with simulated $K_{cb\ SIMDualKc}$ for Godello (Fig. 8a) and Mencía (Fig. 8b) trials. The FTO regression produced $b_0 = 1.01$ for Godello and $b_0 = 1.03$ for Mencía, thus a slight over-estimation, while the resulting error in K_{cb} estimation was RMSE of 0.02 and 0.04 for Godello and Mencía, respectively.

5.2. Vegetable crops

5.2.1. Peas for industry

The data set used was obtained at two commercial fields, one of 30 ha located at Alpiarça and the other with 47 ha at Golegã, central Portugal, both cropped with vining peas for industry during two seasons, 2011–2012, as reported by Paredes et al. (2017). During the first year both fields were monitored, but only one was monitored in the second year. Measurements included the net irrigation depths, soil water content with FDR devices down to 0.80 m, crop height, root depths and $f_{c\ eff}$. Soil water content was measured twice a week along the crop seasons at several representative locations. The fraction of soil shaded by the crop canopy near solar noon was observed within four

Table 3
Ranges in parameters for the A&P approach used in Eqs. (4), (6), (7) and (9) to produce $K_{cb\ A\&P}$ values for Lemon trees.

Crop stages	h (m)[a]	$f_{c\ eff}$[a]	F_r	$K_{cb\ full}$	K_d	$K_{cb\ A\&P}$
Development	3.1–3.5	0.62–0.67	0.65–0.75	0.50–0.83	0.74–0.85	0.54–0.71
Mid-season	3.5–3.7	0.67–0.71	0.75	0.83–0.84	0.85–0.91	0.71–0.77

[a] Field data from Rosa (2019).

Table 4
Ranges in parameters for the A&P approach used in Eqs. (4), (6), (7) and (9) to produce $K_{cb\ A\&P}$ values for wine grapes, bare soil cultivation.

Crop stages	h (m)[a]	$f_{c\ eff}$[a]	F_r	$K_{cb\ full}$	K_d	$K_{cb\ A\&P}$
Initial	1.5	0.11–0.20	0.65	0.78–0.79	0.12–0.22	0.23–0.29
Development	1.5	0.20–0.40	0.65	0.78–0.79	0.22–0.69	0.29–0.61
Mid-season	1.5	0.40–0.45	0.65	0.78–0.79	0.69–0.73	0.61–0.63

[a] Field data from López-Urrea et al. (2012).

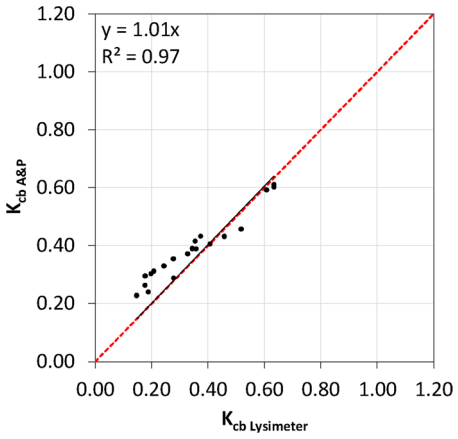

Fig. 6. Linear regression forced through the origin comparing $K_{cb\ A\&P}$ values with $K_{cb\ lysimeter}$ for wine grapes; also depicted is the 1:1 line (- - -) (Field data from López-Urrea et al., 2012).

1 m × 1 m areas at various dates throughout the seasons. In addition, the dates for the crop growth stages were observed. Observations and measurements were used to calibrate and validate the SIMDualKc model. The potential $K_{cb\ SIMDualKc}$ were $K_{cb\ mid} = 1.15$ and $K_{cb\ end} = 1.11$. The high $K_{cb\ end}$ is due to the very early harvest required by the industry.

In the A&P approach $M_L = 2$ was used, and $k_h = 0.2$ in Eq. (6) performed the best in reproducing the $K_{cb\ SIMDualKc}$ data. $k_h = 0.2$ was applied to the pea canopy and for other crops having similar architecture where there is considerable leaf area with relatively low canopy height. Ranges in parameters for the A&P approach used in Eqs. (4), (6), (7) and (9) are given in Table 7. Fig. 9 illustrates the FTO regression between $K_{cb\ A\&P}$ and $K_{cb\ SIMDualKc}$ values. The A&P approach tended to under-estimate the K_{cb} values by about 6 % ($b_0 = 0.94$).

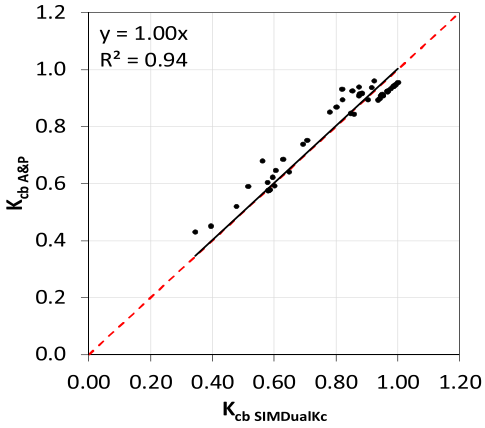

Fig. 7. Linear regression forced through the origin comparing $K_{cb\ A\&P}$ values with $K_{cb\ SIMDualKc}$ for mature Albariño wine grapes in presence of active ground cover; also depicted is the 1:1 line (- - -) (Field data from Fandiño et al., 2012).

5.2.2. Onions

A dataset for onions was reported by López-Urrea et al. (2009a). ET_c measurements of sprinkler-irrigated onions were conducted with a large weighing lysimeter installed in the center of a 100 × 100 m plot. The lysimeter container is 2.7 m long, 2.3 m wide and 1.7 m deep, with an approximate total weight of 14.5 t. The crop inside the lysimeter was kept at the same growth rate as the crop on the outside to minimize edge effects. The lysimeter mass resolution was 0.02 mm, with an accuracy of 0.04 mm equivalent water depth. Readers are referred to López-Urrea et al. (2009a) for a detailed description of lysimeter technical features and measurements. f_c and h values were measured during one growing season, with 34 observations.

A value for $M_L = 2$ was used and $K_{cb\ full}$ was computed with Eq. (6) using $k_h = 0.2$. Table 8 presents ranges for terms of the A&P approach computed using observations. Fig. 10 shows the comparison of estimated $K_{cb\ A\&P}$ values with measured $K_{cb\ Lysimeter}$. The slope of the linear regression forced through the origin shows a slight under-estimation tendency with $b_0 = 0.96$.

5.2.3. Tomato

A dataset for tomato refers to a study by Zheng et al. (2013). Field experiments were developed during 2010 and 2011 seasons at Wuwei, Gansu province, Northwest China. Five drip-irrigated treatments relative to various soil matric potential thresholds were considered using a completely randomized design. Measurements included root depths, leaf area index (LAI), precipitation, net irrigation depths and soil water content surveyed down to 0.80 m. Tomato ET was derived from the soil

Table 5
Ranges in parameters for the A&P approach used in Eqs. and (4), (5), (6), (7) and (9) to produce $K_{cb\ A\&P}$ values for Albariño vineyard with active ground cover based upon 5 years of field observations, 2008–2012.

Crop stages	h (m)[a]	$f_{c\ eff}$[a]	$f_{c\ gcover}$[a]	F_r	$K_{cb\ full}$	$K_{cb\ gcover}$	K_d	$K_{cb\ A\&P}$
Initial	2.0	0.11–0.16	0.60–0.80	0.90	1.02–1.04	0.36–0.56	0.17–0.24	0.52–0.64
Development	2.0	0.15–0.58	0.65–0.83	0.90	1.02–1.04	0.16–0.65	0.24–0.83	0.43–0.89
Mid-season	2.0	0.58–0.70	0.50–0.65	0.90	1.02–1.06	0.15–0.58	0.84–0.89	0.89–0.96
Late-season	2.0	0.70–0.56	0.65–0.85	0.85	1.02–0.92	0.18–0.83	0.87–0.82	0.92–0.84

[a] Field data from Fandiño et al. (2012).

Table 6
Ranges in parameters for the A&P approach used in Eqs. and (4), (5), (6), (7) and (9) to produce $K_{cb\ A\&P}$ values for Godello and Mencía vineyards with initially active ground cover that later mulched.

Crop stages	h (m)[a]	$f_{c\ eff}$[a]	$f_{c\ gcover}$[a]	F_r	$K_{cb\ full}$	$K_{cb\ gcover}$	K_d	$K_{cb\ A\&P}$
Godello								
Development	1.20–1.25	0.15–0.20	0.70–0.80	0.70	0.74–0.78	0.19–0.32	0.23–0.30	0.36–0.42
Mid-season	2.00	0.25–0.30	~ 0.50	0.70	0.83	0.19	0.38–0.45	0.43–0.48
Late-season	2.00	0.30–0.25	~ 0.50	0.50	0.83–0.60	0.19	0.45–0.38	0.48–0.34
Mencía								
Development	1.50–1.90	0.15–0.35	0.60–0.80	0.20–0.68	0.20–0.80	0.15–0.57	0.08–0.53	0.28–0.54
Mid-season	1.90–2.00	0.25–0.47	0.40–0.60	0.65–0.68	0.74–0.80	0.15–0.28	0.38–0.55	0.42–0.53
Late-season	1.40–2.00	0.25–0.48	0.40–0.60	0.50–0.53	0.58–0.61	0.15–0.27	0.38–0.73	0.34–0.49

[a] Field data from Cancela et al. (2015).

water balance.

K_d was obtained from LAI measurements performed during two growing seasons using Eq. (8). $K_{cb\ full}$ was computed with Eq. (6) using $k_h = 0.1$ because, differently from other vegetable crops referred before, the crop was trained on a trellis. Table 9 presents ranges for the terms of the A&P approach computed using LAI and h observations. Fig. 11 shows the comparison of single crop coefficients, the estimated $K_{c\ A\&P}$ values and $K_{c\ SWB}$ derived from soil water balance observations. The slope of the linear FTO regression produced $b_0 = 1.00$, indicating no tendency for under- or over-estimation.

5.3. Field crops

5.3.1. Barley

Data sets were collected along two contrasting rainfall seasons, 2012 and 2013, at a 30 ha commercial malting barley field located at Alpiarça, central Portugal (Pereira et al., 2015). Measurements included root depths, crop height, LAI, $f_{c\ eff}$, net irrigation depths and soil water content. The latter were measured with FDR devices to a depth of 0.90 m. Observations were performed at several representative locations within the field. The dates of the crop growth stages were observed along both seasons. All observations and measurements were used to properly calibrate and validate the SIMDualKc model and therefore to derive adequate K_{cb} values. The potential $K_{cb\ SIMDualKc}$ was set to $K_{cb\ mid} = 1.04$ and $K_{cb\ end} = 0.10$ based on ET measurement data.

$M_L = 2$ was used and the best-fit k_h value was 0.1. Table 10 provides ranges for parameters used with the A&P approach. Fig. 12 presents the FTO regression relating the $K_{cb\ SIMDualKc}$ with the $K_{cb\ A\&P}$ values, which produced $b_0 = 1.02$, which was close to 1.

5.3.2. Wheat

Three sets of data were evaluated for wheat. One set represented winter wheat with frozen soil after sowing, and two sets represented spring wheat. The winter wheat study was performed along two seasons (2007 – 08 and 2008 – 09) in Daxing, North China Plain (Zhao et al., 2013; Zhang et al., 2013). Field observations to obtain crop ET and to calibrate and validate the SIMDualKc model included the soil water content using TDR devices along the entire root zone (1.0 m) and EC observations. In addition, observations also included crop height, root depths, the fraction of ground cover (f_c) observed randomly along the crops' season, soil evaporation measured with microlysimeters placed

Table 7
Ranges in parameters for the A&P approach used in Eqs. (4), (6), (7) and (9) to produce $K_{cb\ A\&P}$ values for peas for the industry.

Crop stages	h (m)[a]	$f_{c\ eff}$[a]	F_r	$K_{cb\ full}$	K_d	$K_{cb\ A\&P}$
Mid-season	0.45–0.50	0.97–1.00	1.0	1.06–1.08	0.98–1.00	1.06–1.08
End-season	0.45–0.50	0.99–1.00	1.0	1.05–1.07	0.99–1.00	1.05–1.07

[a] Field data from Paredes et al. (2017).

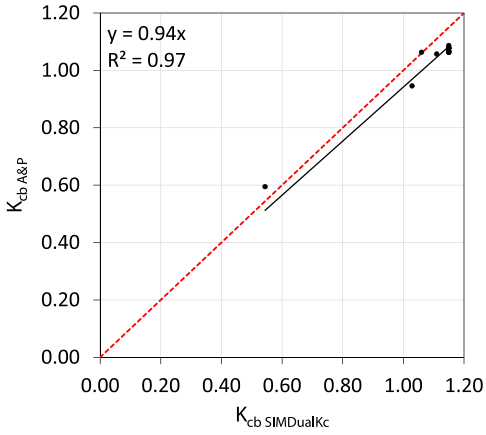

Fig. 9. Linear regression forced through the origin comparing $K_{cb\ A\&P}$ values with $K_{cb\ SIMDualKc}$ for vining peas; also depicted is the 1:1 line (- - -) (Field data from Paredes et al., 2017).

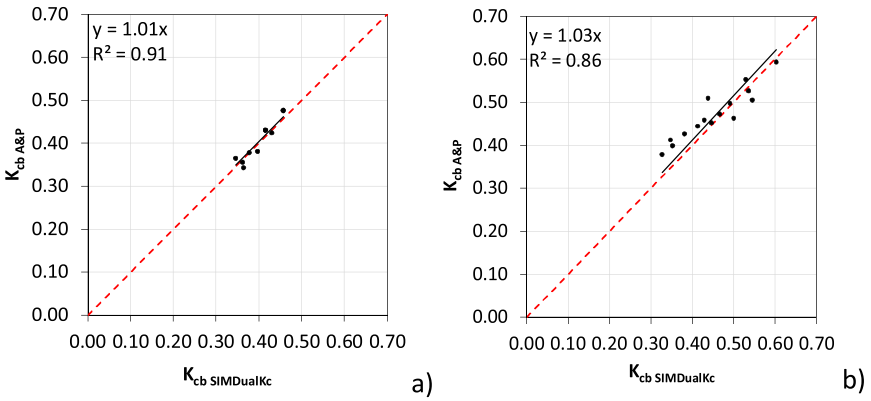

Fig. 8. Linear regression forced through the origin comparing $K_{cb\ A\&P}$ values with $K_{cb\ SIMDualKc}$ in presence of active ground cover for a) mature Godello wine grapes and b) mature Mencía wine grapes; also depicted is the 1:1 line (- - -) (Field data from Cancela et al., 2015).

Table 8
Ranges in parameters for the A&P approach used in Eqs. (4), (6), (7) and (9) to produce $K_{cb\ A\&P}$ values for onions.

Crop stages	h (m)[a]	$f_{c\ eff}$[a]	F_r	$K_{cb\ full}$	K_d	$K_{cb\ A\&P}$
Initial	0.10–0.18	0.02–0.13	1.0	1.06–1.09	0.02–0.18	0.17–0.32
Development	0.19–0.40	0.16–0.69	1.0	1.09–1.17	0.18–0.76	0.32–0.92
Mid-season	0.39–0.40	0.68–0.74	1.0	1.17	0.76–0.80	0.92–0.97
Late-season	0.21–0.34	0.21–0.54	1.0	1.17–1.11	0.76–0.27	0.97–0.41

[a] Field data from López-Urrea et al. (2009a).

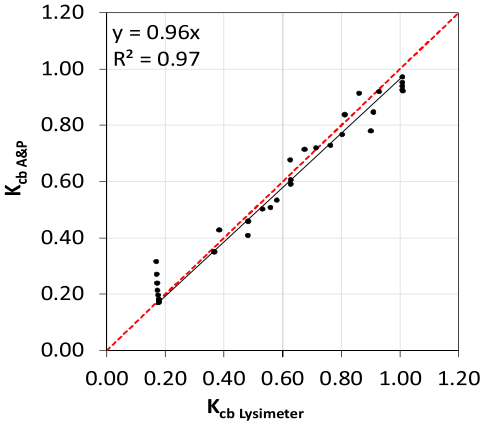

Fig. 10. Linear regression forced through the origin comparing $K_{cb\ A\&P}$ values with $K_{cb\ Lysimeter}$ for onions; also depicted is the 1:1 line (- - -) (Field data from López-Urrea et al., 2009a).

along the crop row, the dates of the crop growth stages, and the net irrigation depths.

One of the spring wheat data sets was observed at Hetao, Inner Mongolia (Miao et al., 2016), where the wheat was sown after frozen soil melting. This study was performed during three seasons (2010–2012) and various basin irrigated fields were surveyed with the soil water content measured with the gravimetric method. Field observations and measurements performed at randomly distributed locations within each 10 × 50 m plot included crop height, f_c, the dates of the crop growth stages, the rooting depth, net irrigation depths and precipitation. Wheat ET was obtained from the soil water balance with the SIMDualKc calibrated and validated against soil water content data, therefore making it appropriate to derive K_{cb} from observations of the SWB.

The third set for spring wheat was sowed in a semi-arid environment near Albacete, Spain, and K_{cb} were obtained with weighing lysimeters (Sánchez et al., 2015). The dual crop coefficient was calculated with the standard FAO56 approach (Allen et al., 1998) and using the crop coefficient values obtained from lysimeter measurements. First, the evaporation component (K_e) was calculated with the FAO56 methodology and, afterwards, the basal crop coefficient (K_{cb}) was obtained from the lysimeter K_c values minus the calculated K_e values. The lysimeter description is provided in Section 5.2.2. and additional information is given in López-Urrea et al. (2009b) and Sánchez et al. (2015). For winter wheat the potential $K_{cb\ SIMDualKc}$ values fitted to ET measurements were $K_{cb\ mid}$ = 1.14 and $K_{cb\ end}$ = 0.25, while for spring wheat the fitted potential $K_{cb\ SIMDualKc}$ values were $K_{cb\ mid}$ = 1.15 and

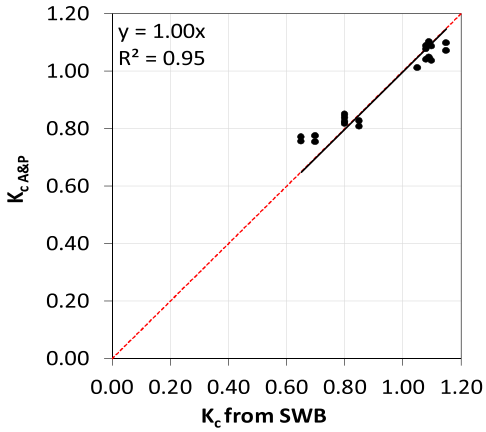

Fig. 11. Linear regression forced through the origin comparing $K_{c\ A\&P}$ values with $K_{c\ SWB}$ for tomato; also depicted is the 1:1 line (- - -) (Field data from Zheng et al., 2013).

$K_{cb\ end}$ = 0.32 in Hetao and $K_{cb\ mid}$ = 1.15 and $K_{cb\ end}$ = 0.21 in Albacete.

For all cases, a M_L = 2 was used and the best fit k_h used in Eq. (6) was 0.2. Table 11 provides for the parameters used with the A&P approach for the three case studies. Fig. 13 presents the FTO regression relating $K_{cb\ A\&P}$ with $K_{cb\ SIMDualKc}$ or $K_{cb\ Lysimeter}$ for both winter and spring wheat. A slight tendency for under-estimation of $K_{cb\ A\&P}$ for the winter wheat crop (b_0 = 0.95) was observed, but not for spring wheat cases (b_0 = 1.00 and 0.98 respectively for China and Spain case studies).

5.3.3. Maize

Several data sets were used for evaluation of the A&P approach for maize. Studies for non-stressed grain maize are reported by Zhang et al. (2013) and Zhao et al. (2013) relative to experiments in Daxing, North China Plain, where ET_{EC} and ET from a SWB were observed and K_{cb} were derived from the respective calibration and validation of SIMDualKc. Other studies using a SWB are those reported by Martins et al. (2013) using FDR instrumentation in Santa Maria, southern Brazil, by Paredes et al. (2014) also using FDR in Alpiarça, central Portugal, and by Miao et al. (2016) in Hetao, Inner Mongolia, using the gravimetric method. A rainfed groundwater-dependent grain maize was studied in Horqin, Eastern Inner Mongolia, where a SWB was used to derive crop ET under water stress conditions as reported by Wu et al. (2015a). In addition, a study on grain maize subject to high levels of water stress reported by Giménez et al. (2016) was developed at Paysandú, western Uruguay, using a SWB supported by neutron probe data. A data set relative to a SWB observed with silage maize cropped at Santa Maria, southern Brazil, was reported by Martins et al. (2013), which refers to the use of FDR measurements. For most cases, experiments were performed during two seasons. Measurements included, for all cases, the components of the soil water balance which were used to properly calibrate and validate the SIMDualKc model and therefore to derive K_{cb}. The soil evaporation was also measured in the study by Zhao et al. (2013).

M_L was set to 2 for the non-water stress data sets and 1.5 for the water stressed data set, which produced a smaller canopy density. For

Table 9
Ranges in parameters for the A&P approach used in Eqs. (4), (6), (7) and (8) to produce basal $K_{cb\ A\&P}$ and single $K_{c\ A\&P}$ values for tomato trained on trellis.

Crop stages	h (m)[a]	LAI[a]	F_r	$K_{cb\ full}$	K_d	$K_{cb\ A\&P}$	$K_{c\ A\&P}$
Mid-season	0.42–0.69	3.7–7.3	1.0	1.02–1.07	0.92–0.99	0.96–1.05	1.01–1.10
End-season	0.42–0.69	2.3–4.0	0.8	0.82–0.85	0.80–0.94	0.70–0.80	0.75–0.85

[a] Field data from Zheng et al. (2013).

Table 10
Ranges in parameters for the A&P approach used in Eqs. (4), (6), (7) and (9) to produce $K_{cb\ A\&P}$ values for malt barley.

Crop stages	h (m)[a]	$f_{c\ eff}$[a]	F_r	$K_{cb\ full}$	K_d	$K_{cb\ A\&P}$
Mid-season	0.75–0.80	0.82–0.93	1.00	1.05	0.88–0.96	0.94–0.98
Late-season	0.60–0.75	0.65–0.82	1.00–0.30	0.32–1.05	0.78–0.96	0.29–0.98
End-season	0.60–0.62	0.65–0.70	0.30	0.32–0.52	0.78–0.81	0.29–0.44

[a] Field data from Pereira et al. (2015).

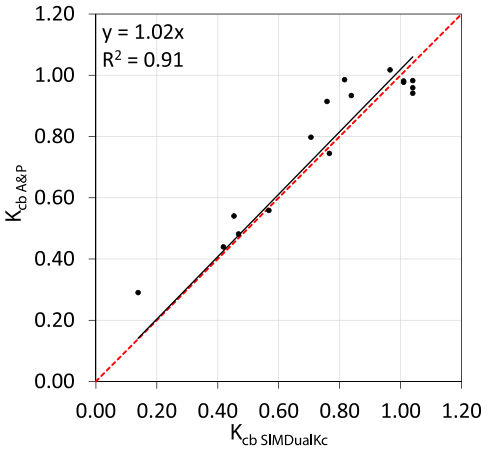

Fig. 12. Linear regression forced through the origin comparing $K_{cb\ A\&P}$ values with $K_{cb\ SIMDualKc}$ for barley; also depicted is the 1:1 line (- - -) (Field data from Pereira et al., 2015).

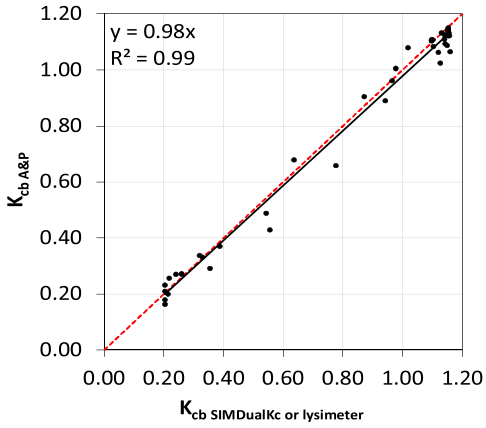

Fig. 13. Linear regression forced through the origin comparing wheat $K_{cb\ A\&P}$ values with those derived with SIMDualKc or from lysimeter ($K_{cb\ SIMDualKc\ or\ lysimeter}$); also depicted is the 1:1 line (- - -) (Field data from Sánchez et al., 2015; Zhao et al., 2013; and Miao et al., 2016).

all cases, the best k_h value was 0.1. For grain maize, the potential $K_{cb\ SIMDualKc}$ for $K_{cb\ mid}$ ranged from 1.10 to 1.17 and the $K_{cb\ end}$ ranged from 0.26 to 0.38 depending upon the grain moisture at harvest. Lower $K_{cb\ SIMDualKc}$ were obtained for the rainfed maize at Horqin, with $K_{cb\ mid}$ = 0.95 and $K_{cb\ end}$ = 0.15. For the high water stress Uruguayan case, $K_{cb\ mid}$ ranged from 1.00–1.08 and $K_{cb\ end}$ was 0.36. For silage maize $K_{cb\ mid}$ was 1.11 and $K_{cb\ end}$ was 0.77.

Table 12 provides ranges for parameters used with the A&P approach. F_r was set to 0.65 for the end season for silage maize, indicating impacts of some leaf senescence and reduction in stomatal conductance; whereas for the end season of grain maize F_r was set to 0.45 when harvesting with high grain moisture, and 0.30 when harvesting with low grain moisture. The reduction in F_r was necessary during late season to counteract the impact of relatively high f_c, even though leaves were senescing. Fig. 14 presents the FTO regression relating $K_{cb\ SIMDualKc}$ with $K_{cb\ A\&P}$ for the various cases. Results show no tendency for under- or over-estimation with b_0 values close to 1.0 for individual cases. Fig. 14 presents the regression relating $K_{cb\ A\&P}$ with $K_{cb\ SIMDualKc}$ for all maize data sets, with results (b_0 = 1.01) showing that the A&P approach presented no tendencies for under- or over-estimating observed $K_{cb\ SIMDualKc}$ values.

5.3.4. Sunflower

Two data sets were available for sunflower. One refers to three seasons (2010–2012) of field studies near Hetao, Inner Mongolia, as described by Miao et al. (2016). Sunflower ET was derived from a SWB based upon gravimetric method data. Measurements were used to properly calibrate and validate the SIMDualKc model. The potential $K_{cb\ SIMDualKc}$ values were $K_{cb\ mid}$ = 1.16 and $K_{cb\ end}$ = 0.27. The second dataset refers to weighing lysimeter studies performed during two growing seasons near Albacete, Spain, as reported by López-Urrea et al. (2014). In this study sunflower ET_c measurements were conducted with a large weighing lysimeter previously described. The basal crop coefficient (K_{cb}) was obtained from the lysimeter K_c values minus the calculated K_e values using the FAO56 methodology (Allen et al., 1998).

M_L = 2 was adopted, with a best-fit k_h value of 0.1. Table 13

Table 11
Ranges in parameters for the A&P approach used in Eqs. (4), (6), (7) and (9) to produce $K_{cb\ A\&P}$ values for winter and spring wheat.

Crop stages	h (m)[a]	$f_{c\ eff}$[a]	F_r	$K_{cb\ full}$	K_d	$K_{cb\ A\&P}$
Winter wheat						
Mid-season	0.75–0.77	0.91	1.00	1.12–1.14	0.95	1.06–1.09
Late-season	0.70–0.77	0.64–0.91	0.35–1.00	0.39–1.14	0.77–0.95	0.33–1.09
End-season	0.70	0.64	0.35	0.39	0.77	0.33–0.34
Spring wheat, Hetao						
Mid-season	0.82–0.84	0.89–0.91	1.00	1.17–1.18	0.94–0.95	1.11–1.13
Late-season	0.80–0.84	0.40–0.91	0.30–1.00	0.34–1.18	0.60–0.95	0.27–1.13
End–season	0.80–0.81	0.40–0.43	0.30	0.34–0.35	0.60–0.63	0.27
Spring wheat, Albacete						
Initial	0.04–0.08	0.02–0.12	0.70–0.80	0.72–0.81	0.02–0.14	0.16–0.23
Development	0.08–0.46	0.12–0.86	0.80–1.00	0.81–1.13	0.14–0.91	0.23–1.08
Mid-season	0.46–0.68	0.86–0.97	1.00	1.13–1.18	0.91–0.98	1.08–1.15
Late-season	0.68–0.60	0.97–0.03	1.00–0.80	1.18–0.93	0.98–0.06	1.15–0.20

[a] Winter wheat field data from Zhao et al. (2013) and Zhang et al. (2013); Spring wheat data from Miao et al. (2016) and Sánchez et al. (2015).

Table 12
Ranges in parameters for the A&P approach used in Eqs. (4), (6), (7) and (9) to produce $K_{cb\ A\&P}$ values for grain and silage maize with and without water stress.

Crop stages	h (m)[a]	$f_{c\ eff}$[a]	F_r	$K_{cb\ full}$	K_d	$K_{cb\ A\&P}$
Grain maize						
High moisture at harvesting						
Mid-season	2.50	0.86	1.00	1.11–1.12	0.96	1.07–1.08
Late-season	2.30–2.50	0.54–0.86	0.45–1.00	0.51–1.12	0.83–0.96	0.45–1.08
End-season	2.30	0.54	0.45	0.51	0.83	0.45
Low moisture at harvesting						
Mid-season	1.95–2.80	0.83–0.99	1.00	1.11–1.19	0.94–1.00	1.07–1.18
Late-season	1.90–2.80	0.43–0.99	0.30–1.00	0.34–1.19	0.75–1.00	0.31–1.18
End-season	1.90–2.70	0.43–0.73	0.30	0.34–0.40	0.75–0.91	0.31–0.36
Water stressed						
Mid-season	1.70–2.00	0.66–0.93	0.90	1.03–1.08	0.91–0.99	0.94–1.07
Late-season	1.60–2.00	0.50–0.93	0.27–0.90	0.30–1.08	0.86–0.99	0.28–1.07
End-season	1.60–1.95	0.50–0.90	0.27	0.30–0.31	0.86–0.97	0.28–0.30
Silage maize						
Mid-season	2.20–2.40	0.85–0.95	1.00	1.17	0.95–0.99	1.12–1.15
Late-season	2.20–2.40	0.85–0.95	0.65–1.00	0.75–1.17	0.95–0.99	0.72–1.15
End-season	2.20–2.40	0.85–0.95	0.65	0.75	0.95–0.99	0.72–0.74

[a] Field data from Zhao et al. (2013) and Zhang et al. (2013) for grain maize with high moisture; Martins et al. (2013) and Paredes et al. (2014) for grain maize with low moisture at harvesting; Wu et al. (2015a) and Giménez et al. (2016) for grain maize with water stress; Martins et al. (2013) for silage maize.

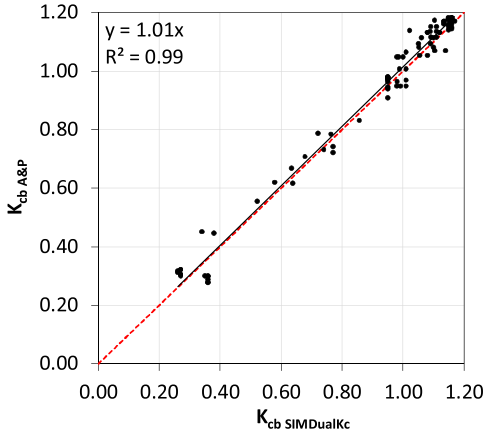

Fig. 14. Linear regression forced through the origin comparing $K_{cb\ A\&P}$ values with $K_{cb\ SIMDualKc}$ for all the data sets relative to maize; also depicted is the 1:1 line (- - -) (Field data from Martins et al., 2013; Zhao et al., 2013; Paredes et al., 2014; Wu et al., 2015a; Giménez et al., 2016; and Miao et al., 2016).

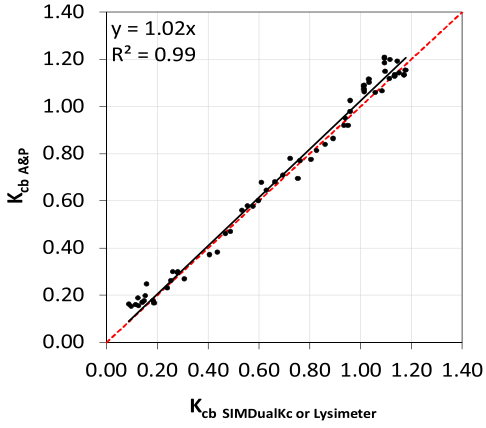

Fig. 15. Linear regression forced through the origin comparing sunflower $K_{cb\ A\&P}$ values with those derived from SIMDualKc or from lysimeter ($K_{cb\ SIMDualKc\ or\ lysimeter}$); also depicted is the 1:1 line (- - -) (Field data from López-Urrea et al., 2014, and Miao et al., 2016).

provides ranges for values for parameters used with the A&P approach. The regression results relating $K_{cb\ A\&P}$ values with $K_{cb\ SIMDualKc}$ or $K_{cb\ lysimeter}$ produced $b_0 = 0.99$ and 1.03 respectively for the China and Spain case studies. Combining all sunflower datasets resulted in $b_0 = 1.02$ (Fig. 15), thus a slight tendency for over-estimation.

5.3.5. Canola

The canola dataset represented a one-year experiment with weighing lysimeters reported by Sánchez et al. (2014). ET_c measurements of sprinkler-irrigated canola were carried out with a weighing lysimeter located at the lysimeter facility near Albacete (southeast Spain). K_{cb} values were determined from the lysimeter K_c values (lysimeter ET_c/PM-ET_o) minus the calculated K_e values using the FAO56 approach (Allen et al., 1998).

An $M_L = 2$ was used and the best-fit k_h was 0.1. Table 14 presents ranges in terms of the A&P approach computed using observations. Fig. 16 shows the comparison of estimated $K_{cb\ A\&P}$ values with measured $K_{cb\ Lysimeter}$. The slope of the linear FTO regression was 0.99, thus

Table 13
Ranges in parameters for the A&P approach used in Eqs. (4), (6), (7) and (9) to produce $K_{cb\ A\&P}$ values for sunflower.

Crop stages	h (m)[a]	$f_{c\ eff}$[a]	F_r	$K_{cb\ full}$	K_d	$K_{cb\ A\&P}$
China						
Mid-season	1.94–1.96	0.87–0.90	1.00	1.17–1.19	0.95–0.96	1.12–1.14
Late-season	1.89–1.96	0.40–0.90	1.00–0.30	0.35–1.19	0.73–0.96	0.29–1.14
End-season	1.89–1.93	0.40–0.41	0.30	0.35	0.73–0.75	0.29–0.30
Spain						
Initial	0.05–0.37	0.02–0.17	0.30	0.31–0.33	0.02–0.28	0.15–0.18
Development	0.37–1.41	0.17–0.69	0.30–0.90	0.33–1.21	0.28–0.86	0.18–1.06
Mid-season	1.41–1.61	0.69–0.84	1.00	1.21–1.26	0.86–0.95	1.06–1.21
Late-season	1.61–1.20	0.84–0.09	1.00–0.30	1.26–0.35	0.95–0.19	1.21–0.19

[a] Field data from Miao et al. (2016) and López-Urrea et al. (2014) respectively for Hetao, China and Albacete, Spain.

very close to 1.0.

5.3.6. Cotton

The cotton data set was comprised of two years of observations in Fergana, Central Asia (Cholpankulov et al., 2008), which were used to calibrate and validate the SIMDualKc and to derive appropriate K_{cb} values as described by Rosa et al. (2012b). Measurements included the soil water balance components based upon neutron probe observations. The potential $K_{cb\ SIMDualKc}$ were $K_{cb\ mid} = 1.15$ and $K_{cb\ end} = 0.50$.

The M_L value of 1.5 was adopted and the best k_h value was 0.20. Table 15 provides ranges in parameters used with the A&P approach. The FTO regression relating $K_{cb\ SIMDualKc}$ with $K_{cb\ A\&P}$ values (Fig. 17) produced $b_0 = 0.98$, thus quite close to 1, and indicating the ability to reproduce measurement fitted K_{cb} values using the A&P approach with physically and visually-derived field parameters.

5.3.7. Soybean

Two different sets of data on soybean were evaluated. The first is from Paysandú, eastern Uruguay (Giménez et al., 2017) developed along two seasons, where the soybean varieties are tall, reaching 1.20 m height; in contrast, the second soybean study, developed along three seasons in Daxing, North China Plain (Wei et al., 2015), used a short variety, with an average maximum height of 0.70 m. Measurements included, in both cases, the $f_{c\ eff}$, the dates of the crop growth stages as well as the components of the soil water balance, the former based upon neutron probe observations and on TDR the second. The SWB were used to properly calibrate and validate the SIMDualKc model. The study by Wei et al. (2015) also provided soil evaporation data, which allowed further validation of the ET partition approach used by the SIMDualKc model. The potential $K_{cb\ SIMDualKc}$ for the tall variety fitted to field measurements was $K_{cb\ mid} = 1.10$ and $K_{cb\ end} = 0.42$ while for the short variety, $K_{cb\ mid} = 1.00$ and $K_{cb\ end} = 0.33$. Consequently, different approaches were used when computing $K_{cb\ A\&P}$.

$M_L = 2$ was utilized for both cases and the best-fit k_h value was 0.10. Table 16 provides ranges in parameters used with the A&P approach. The FTO regression relating $K_{cb\ A\&P}$ values with $K_{cb\ SIMDualKc}$ shows b_0 of 0.99 and 0.95 for the data sets of the tall and the short varieties. Combining all the soybeans datasets produced $b_0 = 0.96$ (Fig. 18), thus showing a slight tendency for under-estimation.

5.4. Pasture and forage crops

5.4.1. Grassland

A data set produced from a groundwater-dependent grassland observed during two seasons (2009 and 2011) in the steppe of Horqin, eastern Inner Mongolia, China (Wu et al., 2015b) was evaluated. Killing frosts occurred during both Autumn and Winter. Observations and measurements were performed at random locations and included root depth, f_c, grass height, the dates of the crop growth stages, water table depths, precipitation and the soil water content down to 0.60 m. All information was used to properly calibrate and validate the SIMDualKc model. The potential $K_{cb\ SIMDualKc}$ values fitted to measured $ET_{SIMDualKc}$ were $K_{cb\ mid} = 0.67$ and $K_{cb\ end} = 0.38$; these values are quite low and correspond to cropping under water stress conditions and its effect on vegetation growth and density.

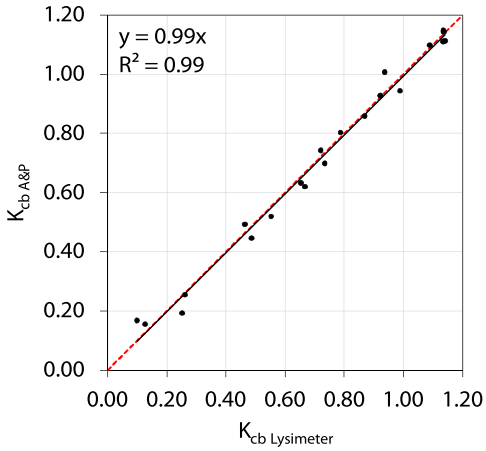

Fig. 16. Linear regression forced through the origin comparing $K_{cb\ A\&P}$ values with $K_{cb\ Lysimeter}$ for canola; also depicted is the 1:1 line (- - -) (Field data from Sánchez et al., 2014).

An M_L value of 1.5 was used, and the best-fit k_h value was 0.20. $F_r < 1.0$ was assumed because the studied steppe grassland was water stressed quite often throughout the cropping season. Table 17 provides ranges in values for parameters used with the A&P approach. The FTO regression relating $K_{cb\ SIMDualKc}$ with $K_{cb\ A\&P}$ values (Fig. 19), shows a good agreement ($b_0 = 1.01$).

5.4.2. Bermudagrass

A data set describing a Tifton bermudagrass cropped in Santa Maria, Brazil, along two growing seasons and two years (2015−16 and 2016−17), was reported by Paredes et al. (2018). The data set consists of three irrigated treatments where the forage cuts were spaced at 124, 248 and 372 cumulative growing degree days (CGDD). Field observations and measurements included: the dates of the crop growth stages relative to the various cuts; net irrigation depths; root depths and grass height; the fraction of ground cover; and the soil water content along the entire root zone of 0.50 m observed with FDR devices. Thus, grass ET was obtained from SWB and the collected data were used to calibrate and validate the SIMDualKc model. The derived potential fitted $K_{cb\ SIMDualKc}$ values were 0.91 and 0.96 respectively for the growth and cutting stages.

$M_L = 1.5$ was applied and the best-fit k_h value was 0.10. Table 18 provides parameters used with the A&P approach. Fig. 20 shows the $K_{cb\ A\&P}$ values compared with the dynamics of the $K_{cb\ SIMDualKc}$ values for two years relative to the case where the interval between successive cuttings was 248 CGDD. The regression between $K_{cb\ A\&P}$ and $K_{cb\ SIMDualKc}$ values was not performed because the range of variation in those values was too small, producing a small R^2 and non-representative b_0. Instead, the quality of estimates for $K_{cb\ A\&P}$ was assessed through verifying if the potential $K_{cb\ SIMDualKc}$ values for the growth and cutting stages, respectively 0.91 and 0.96, fell within the range of $K_{cb\ A\&P}$ given in Table 18. This assessment can be confirmed through the visual observation of Fig. 20, which shows that $K_{cb\ A\&P}$ fit modelled $K_{cb\ SIMDualKc}$ curves well for forage cuttings at 248 CGDD; results for 124 and 372 CGDD (not shown) were similar.

Table 14
Ranges in parameters for the A&P approach used in Eqs. (4), (6), (7) and (9) to produce $K_{cb\ A\&P}$ values for canola.

Crop stages	h (m)[a]	$f_{c\ eff}$[a]	F_r	$K_{cb\ full}$	K_d	$K_{cb\ A\&P}$
Initial	0.20	0.05	0.20	0.21	0.09	0.16
Development	0.32–0.76	0.16–0.97	0.30–1.00	0.32–1.12	0.25–0.98	0.19–1.11
Mid-season	0.76–1.10	0.97–0.87	1.00	1.12–1.18	0.98–0.94	1.11–1.15
Late-season	1.10–1.00	0.87–0.10	1.00–0.20	1.18–0.24	0.94–0.20	1.15–0.17

[a] Field data from Sánchez et al. (2014).

Table 15
Ranges in parameters for the A&P approach used in Eqs. (4), (6), (7) and (9) to produce $K_{cb\ A\&P}$ values for cotton.

Crop stages	h (m)[a]	$f_{c\ eff}$[a]	F_r	$K_{cb\ full}$	K_d	$K_{cb\ A\&P}$
Mid-season	1.10–1.20	0.81–0.99	1.00	1.17–1.18	0.89–1.00	1.08–1.17
Late-season	1.10–1.20	0.78–0.99	0.35–1.00	0.59–1.18	0.89–1.00	0.54–1.17
End-season	1.10	0.78	0.35	0.59	0.89	0.54

[a] Field data from Cholpankulov et al. (2008).

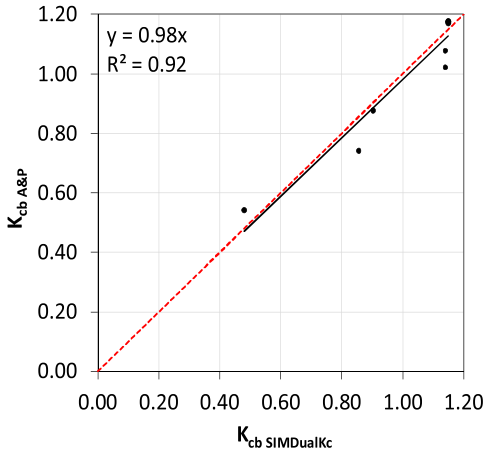

Fig. 17. Linear regression forced through the origin comparing $K_{cb\ A\&P}$ values with $K_{cb\ SIMDualKc}$ for cotton; also depicted is the 1:1 line (- - -) (Field data from Rosa et al., 2012b).

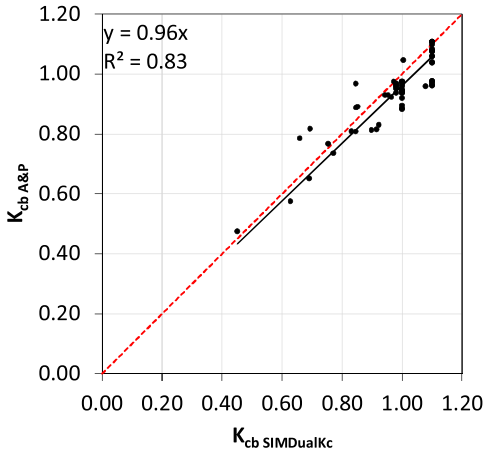

Fig. 18. Linear regression forced through the origin comparing $K_{cb\ A\&P}$ values with $K_{cb\ SIMDualKc}$ for all soybean data sets; also depicted is the 1:1 line (- - -) (Field data from Wei et al., 2015; Giménez et al., 2017).

5.5. Summary of goodness-of-fit indicators

Table 19 presents the goodness of fit indicators used to compare estimated $K_{cb\ A\&P}$ with SIMDualKc model-derived K_{cb} or lysimeter-derived K_{cb} relative to all crops described in the previous sections. These results show that the coefficients of regression for the FTO regression varied between 0.94 and 1.03, which indicates that $K_{cb\ A\&P}$ values are statistically close, on average, to $K_{cb\ SIMDualKc}$ or to $K_{cb\ Lysimeter}$, thus producing estimates for K_{cb} values similar to those resulting from field measurements. Moreover, this similarity of estimates refers not only to $K_{cb\ mid}$ but also to the late season and, despite the fact that the observation period is short, to the crop development stage as well. In addition, similarity was observed not only for crops under pristine cultivation but also for crops under water stress, which effectively expands the scope of application of the A&P approach.

The ordinary least squares (OLS) coefficients of determination were relatively high, generally ≥ 0.90, which indicates that the A&P computed K_{cb} values were quite close to the fitted regression line and the target K_{cb} values produced by the SIMDualKc model. This provides confidence in the ability of predictions from the A&P approach to reproduce field conditions. Associated with the good results for both b_0 and R^2, the RMSE are small, generally much smaller than 10 % of K_{cb}, where 10 % is a commonly accepted or expected error in ET measurement and modelling (Allen et al., 2011).

5.6. A modification of the F_r parameter (Eq. (7)) for tree orchards

The parameter F_r (Allen et al., 1998) applies a downward adjustment ($F_r \leq 1.0$) to $K_{cb\ full}$ when the vegetation exhibits more stomatal control on transpiration than it is common for most annual agricultural crops, which is of particular importance for perennial crops and for the late season of annual crops. The standard value for F_r is 1.0 since for most non-stressed annual crops r_l is approximately 100 s m^{-1}. The applications presented above refer to F_r values not computed from observed r_l values but estimated with a simplified tentative and error procedure aimed at driving the A&P computed K_{cb} values ($K_{cb\ A\&P}$) towards the K_{cb} determined using accurate ET measurement approaches described in the relevant references. Those applications show $F_r < 1.0$ for perennials (Section 5.1) and $F_r = 1.0$ for vegetable and field crops (Sections 5.2 and 5.3), however with $F_r < 1.0$ after senescence started. This empirical parameterization was successfully adopted when tabulating K_{cb} and K_c for a wide panoply of annual and perennial crops (Pereira et al., 2020a) aimed at providing indicative values for the parameters of the A&P approach, F_r included, since K_{cb} and K_c were previously determined (Pereira et al., 2020b, c).

A different approach has been proposed by Mobe et al. (2020) based upon measurements in 12 apple orchards of South Africa, with f_c varying from 0.20 to 0.60, and relative to four apple varieties. After observing that the K_{cb} resulting from the A&P approach ($K_{cb\ A\&P}$) largely overestimated the K_{cb} derived from eddy covariance measurements, Mobe et al. (2020)

Table 16
Ranges in parameters for the A&P approach used in Eqs. (4), (6), (7) and (9) to produce $K_{cb\ A\&P}$ values for soybean.

	Crop stages	h (m)[a]	$f_{c\ eff}$[a]	F_r	$K_{cb\ full}$	K_d	$K_{cb\ A\&P}$
Tall variety	Mid-season	0.87–1.20	1.00	1.00	1.04–1.11	1.00	1.04–1.11
	Late-season	1.05	0.88	0.83	0.86	0.94	0.82
Short variety	Mid-season	0.60–0.74	0.92–0.96	1.00	0.98–1.00	0.95–0.98	0.94–0.98
	Late-season	0.60–0.69	0.90–0.96	1.00–0.30	0.31–1.00	0.94–0.98	0.30–0.98
	End-season	0.69	0.90	0.30	0.31	0.94	0.30

[a] Field data from Giménez et al. (2017) and Wei et al. (2015), for tall and short soybean variety respectively.

Table 17
Ranges in parameters for the A&P approach used in Eqs. (4), (6), (7) and (9) to produce $K_{cb\ A\&P}$ values for a groundwater dependent steppe grassland.

Crop stages	h (m)[a]	$f_{c\ eff}$[a]	F_r	$K_{cb\ full}$	K_d	$K_{cb\ A\&P}$
Mid-season	0.15	0.83–0.97	0.70	0.73–0.75	0.82–0.94	0.64–0.70
Late-season	0.15	0.68–0.97	0.70–0.45	0.47–0.75	0.69–0.94	0.37–0.70
End-season	0.15	0.68–0.78	0.45	0.47–0.48	0.69–0.78	0.37–0.40

[a] Field data from Wu et al. (2015b).

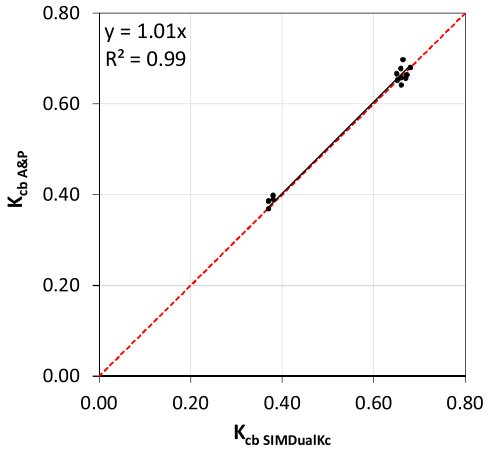

Fig. 19. Linear regression forced through the origin comparing $K_{cb\ A\&P}$ values with $K_{cb\ SIMDualKc}$ for a groundwater dependent grassland cropped in the Mongolian steppe; also depicted is the 1:1 line (- - -) (Field data from Wu et al., 2015b).

found that F_r was over-estimated due to using the ratio $r_l/100$ with the observed apple r_l to the average leaf resistance of annual crops, 100 s m^{-1}. Instead, they replaced the 100 s m^{-1} in Eq. (7) with a resistance parameter α considered to represent the minimum unstressed canopy resistance for apple trees. Following this modification, they observed that $K_{cb\ A\&P}$ was able to match K_{cb} derived from EC measurements quite well over the 12 orchards. The computations were made for the average r_l = 202 s m^{-1} and α = 37 s m^{-1}.Therefore, the Mobe et al. (2020) proposed that the F_r modification may apply when there are observations of leaf resistance of orchard trees so that the parameter α can be estimated. This approach is of great interest when there are observations of r_l and when K_{cb} values are known, which allow one to back calculate F_r and then solve the F_r function for α. More research along these lines is needed.

6. Applications of K_c and K_{cb} estimation from fraction of ground cover and height using remote sensing

6.1. The Satellite Irrigation Management Support framework

A principal strength of the A&P approach is that it provides a robust and standardized method for deriving K_{cb} values for a wide diversity of crops, as illustrated in Section 5 using mostly physical and visual parameters. Combining the A&P approach with the relationships between NDVI and f_c described in Trout et al. (2008) and Johnson and Trout (2012) provides a basis for wide area mapping of crop coefficients from satellite data. The Satellite Irrigation Management Support (SIMS) framework (Melton et al., 2012, 2020) provides one example of the implementation of this approach for satellite mapping of K_{cb} values, and applications of SIMS to date include both irrigation management and monitoring of crop evapotranspiration by water management agencies. Through a partnership between NASA and the California Department of Water Resources (CDWR), SIMS has been implemented over California, and is currently being expanded to provide data for other states in the western U.S.

SIMS can be driven with satellite data from optical multispectral instruments onboard satellites including Landsat 5, Landsat 7, Landsat 8, Sentinel-2A, Sentinel-2B and others. SIMS can be applied with both atmospherically corrected surface reflectance values or top-of-atmosphere reflectance, though use of surface reflectances generally leads to higher accuracy for SIMS estimates for K_{cb} and ET_c. For the comparisons with ground measurements of ET described below, atmospherically corrected surface reflectance data were obtained from the USGS Landsat Collection 1 for the Enhanced Thematic Mapper (ETM+) on Landsat 7 and the Operational Land Imager (OLI) on Landsat 8.

SIMS first calculates NDVI values from the surface reflectance values, and utilizes the relationship described in Trout et al. (2008) to calculate f_c from NDVI following Eq. (10):

$$f_{c\ eff} = 1.26 * NDVI - 0.18 \quad (10)$$

where $f_{c\ eff}$ is the effective fraction of ground covered or shaded by vegetation near solar noon, and NDVI is the normalized difference vegetation index. This equation has been shown to be robust across a range of crop types, although additional refinements or the use of crop specific equations can be applied to further reduce errors in mapping of K_{cb} values. To facilitate use of the SIMS f_c data with the A&P approach, the satellite derived f_c is used as an estimate of $f_{c\ eff}$, and notated as $f_{c\ eff}$ below for consistency with Section 4.

Following the derivation of $f_{c\ eff}$, SIMS calculates K_d values as a function of $f_{c\ eff}$ and crop height (h), following Eq. (9) in Section 4. Crop type information is used to calculate h, and for the U.S., SIMS uses crop type information gridded at 30 m resolution from the USDA Cropland Data Layer (Johnson and Mueller, 2010). SIMS also allows the user to specify crop type information as an input to the model. SIMS uses maximum crop height (h_{max}) values from Table 12 of FAO-56 (Allen et al., 1998), and assumes that for annuals, h starts at zero and increases linearly to a plateau of h_{max} at 0.7 $f_{c\ eff}$, generally regarded as effective full cover. For vineyards and mature orchards, h is set equal to h_{max}. For orchards, an immaturity correction is implemented when $f_{c\ eff} < 0.5$, and h_{max} is reduced by 1 m. No immaturity correction is applied to vineyards, where h is typically set by physical trellis configuration and young vineyards are thus considered to have the same height as mature vineyards for practical purposes. Once the K_d values are determined, SIMS follows the A&P approach to calculate K_{cb} values, including application of F_r to adjust for stomatal regulation for perennial (tree and vine) crops (for details, see Melton et al., 2020).

Table 18
Ranges in parameters for the A&P approach used in Eqs. (4), (6), (7) and (9) to produce $K_{cb\ A\&P}$ values for Tifton bermudagrass.

Crop stages	h (m)[a]	$f_{c\ eff}$[a]	F_r	$K_{cb\ full}$	K_d	$K_{cb\ A\&P}$	$K_{cb\ SIMDualKc}$
Growth	0.17–0.21	0.88–0.92	1.00	0.99–1.00	0.87–0.93	0.88–0.94	0.91
Cutting	0.21–0.33	0.88–0.94	1.00	0.99–1.02	0.93–0.95	0.94–0.98	0.96

[a] Field data from Paredes et al. (2018).

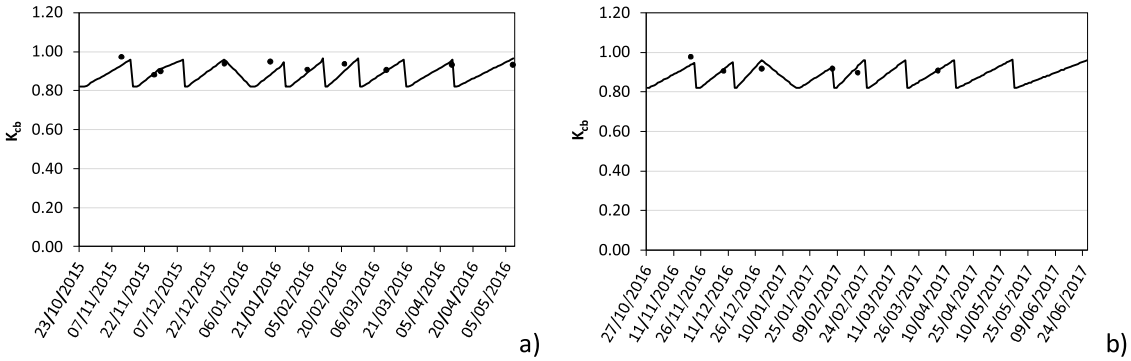

Fig. 20. Comparing $K_{cb\ A\&P}$ values (points) with the $K_{cb\ SIMDualKc}$ (line) for a Tifton Bermudagrass with cuts each 248 cumulative growing degree days, southern Brazil, in a) first and b) second year (Field data from Paredes et al., 2018).

Table 19
Goodness of fit indicators comparing $K_{cb\ A\&P}$ with field derived K_{cb} using the SIMDualKc model ($K_{cb\ SIMDualKc}$) or using weighing lysimeter measurements ($K_{cb\ Lysimeter}$).

Crop	b_0 (FTO)	R^2 (OLS)	RMSE
Perennial crops			
Olives, super-intensive, irrigated	1.00	0.83	0.04
Pears, irrigated	0.98	0.80	0.05
Lemons, irrigated	1.03	0.78	0.06
Wine grapes, irrigated			
without active ground cover	1.01	0.97	0.06
with active ground cover	0.98	0.94	0.07
Vegetable crops			
Peas	0.94	0.97	0.07
Onions	0.96	0.97	0.06
Tomato	1.00	0.95	0.05
Field crops			
Barley	1.02	0.91	0.09
Wheat			
Winter wheat	0.95	0.99	0.06
Spring wheat	0.98	0.99	0.04
All together	0.98	0.99	0.05
Maize crop			
Grain maize, non-stressed	1.02	0.99	0.04
Grain maize, high water-stress	1.00	0.98	0.04
Silage maize, non-stressed	1.02	0.99	0.04
All together	1.01	0.99	0.04
Sunflower	1.02	0.99	0.05
Canola	0.99	0.99	0.04
Cotton	0.98	0.92	0.07
Soybean			
Soybean, short variety	0.95	0.84	0.07
Soybean, tall variety	0.99	0.62	0.05
All together	0.96	0.83	0.07
Pastures and forage crops			
Steppe grassland, groundwater fed	1.01	0.99	0.01
Bermudagrass, irrigated	1.00	–	0.04

FTO refers to the linear regression forced to the origin, OLS refers to the ordinary least squares regression, b_0 is the regression coefficient, R^2 is the coefficient of determination and RMSE is the root mean square error.

SIMS calculates NDVI, $f_{c\ eff}$, and K_{cb} values for each satellite scene, and the time interval is dependent on the satellite data inputs. For the analysis described below, data from Landsat 7 and Landsat 8 were used, resulting in updated values for K_{cb} as frequently as every eight days, excepting cloud cover. Following quality assurance/quality control (QA/QC) procedures and screening for residual cloud cover, K_{cb} values were next linearly interpolated to daily K_{cb} values. Daily grass reference evapotranspiration (ET_o) data were obtained from the California Irrigation Management Information System (CIMIS) operated by CDWR. ET_o data were ingested from Spatial CIMIS, which produces daily ET_o maps for California on a 2 km state-wide grid (Hart et al., 2009). As the final step, daily SIMS crop ET ($ET_{c\text{-}SIMS}$) values are calculated following the FAO56 approach, combining the satellite derived K_{cb} values with the ET_o data from Spatial CIMIS. $ET_{c\text{-}SIMS}$ represents ET from a well-watered crop with minimal soil evaporation, and sets $K_s = 1$ and $K_e = 0$ in Eq. (11).

$$ET_{c\text{-}SIMS} = (K_s K_{cb} + K_e) ET_o \quad (11)$$

In situations where soil evaporation and crop water stress must be considered, SIMS output can be combined with a soil water balance model to facilitate calculation of K_s and K_e based on precipitation records and observed or simulated irrigation events (Melton et al., 2020).

For applications in other states in the U.S., SIMS integrates ET_o data from gridMET (Abatzoglou, 2013) or ET_{ref} data from agricultural weather station networks such as the U.S. Bureau of Reclamation (USBR) AgriMet network, Nevada's NICE Net, or Oklahoma's Mesonet. For international applications, SIMS can be combined with ET_{ref} derived from agricultural weather stations or gridded meteorological fields from global weather models.

A full description of SIMS is available in Melton et al. (2012, 2020), along with an extensive accuracy assessment of $ET_{c\text{-}SIMS}$ data relative to ground-based measurements of ET for a range of crops, including both well-watered and deficit irrigated crops. Since the analyses in this manuscript are primarily focused on K_{cb} values, we summarize results from the accuracy assessment for sites and date ranges that are primarily associated with the well-watered conditions that are best represented by $ET_{c\text{-}SIMS}$.

6.2. Accuracy assessment

Melton et al. (2020) compared $ET_{c\text{-}SIMS}$ with ground-based ET datasets for 14 crop types, under both well-irrigated and deficit-irrigated conditions. Across all crop types studied, they found that SIMS seasonal total ET estimates were within 15 % mean absolute error (MAE) relative to ground-based ET datasets collected in commercial agricultural fields. Use of a soil water balance model to correct for soil evaporation and crop water stress reduced this seasonal error to less than 10 % MAE. On a daily time-step, MAE was 0.4 to 1.0 mm d^{-1} for typically well-watered crops including rice, leaf lettuce, broccoli, and other field crops, and 0.8 to 1.6 mm d^{-1} for deficit irrigated crops, including wine grapes and cotton. Here we evaluate only the subset of the full dataset that can be considered to represent well-watered conditions with a generally dry surface and limited soil evaporation. We extracted the subset based on soil water potential measurements collected at each site, and satellite-derived $f_{c\ eff}$ data to limit the analysis to periods when conditions could be considered to be well-watered, and the crop canopy was established enough to limit soil evaporation relative to the overall ET.

ET ground-based datasets were collected using both flux towers with micrometeorological instrumentation as well as sensor networks and instrumentation used to calculate a complete soil water balance. The flux towers included in the study were instrumented to derive ET either by the full eddy covariance (EC) method or as the residual of the

energy balance (REB). The sites with full EC instrumentation included a peach site and a second wine grape site (*wine2*), and details for these sites are described in Semmens et al. (2016) and Anderson et al. (2017), respectively. Instrumentation deployed at these sites included a 3D sonic anemometer co-located with an open-path gas analyzer, a four-component net radiometer, soil heat flux plates coupled with thermocouples, and humidity and temperature sensors. The REB instrumentation deployed at the first wine grape site (*wine1*) included a similar instrumentation package, with the exception that it did not include an open-path gas analyzer, and calculated the latent energy flux as the residual of the energy balance, following the approach described by Linquist et al. (2015). Instrumentation was deployed at these sites to calculate a daily soil water balance, and included flow meters to measure applied irrigation, precipitation gauges to measure rainfall, capacitance probes and capacitance/frequency domain probes to measure volumetric water content, dielectric water potential sensors to measure soil water potential, and capillary lysimeters to measure drainage below the root zone. For this analysis, daily estimates of actual crop ET were calculated from the micrometeorological instrumentation via energy balance calculations ($ET_{c\ EB}$) and were filtered to eliminate dates when fractional cover was low ($f_{c\ eff} < 25$ %) and when soil water potential (SWP) measured in the field with dielectric soil water potential instruments (MPS-2, Meter Group, Pullman, WA, USA) was less than −100 kPa, indicating sustained soil water deficits.

For annual crops, the daily MAE between $ET_{c\text{-}SIMS}$ and $ET_{c\ EB}$ was 0.71 mm d^{-1} (16.0 %) and the mean bias error (MBE) was 0.33 mm d^{-1} (5.7 %) (Fig. 21). In general there was a strong relationship between $ET_{c\text{-}SIMS}$ and $ET_{c\ EB}$ (R^2 = 0.81), and the largest differences were associated with the rice crop and explained by flood irrigation events that substantially increased evaporation even with a well-established canopy. For the perennial crop sites evaluated, MAE was 0.67 mm d^{-1} (21.7 %), MBE was 0.35 mm d^{-1} (6.9 %) and R^2 was 0.91 (Fig. 22). While these data represent only eight of the hundreds of different crops grown in California, the crops included in this analysis span a wide range of growth forms and include examples of flood, sprinkler and drip irrigated crops. Overall, the results demonstrate the utility of the A&P approach to provide valuable information for irrigation scheduling and management that is representative of well-watered conditions, and provide an indication of the error that might be associated with use of K_{cb} values derived from satellite data in combination with ET_{ref} data provided by agricultural weather networks. SIMS currently provides data for California via web-based data services, which provide capabilities for visualization of maps and time series, as well as data retrieval via an application programming interface (API). SIMS is available as open source code, and includes both a python implementation for use on local or cloud-based computing resources, and as an implementation on Google's Earth Engine (Gorelick et al., 2017) using the python API for Earth Engine. The SIMS API is being used to integrate data from SIMS into other irrigation management software, including Irriquest (Johnson et al., 2014) and CropManage (Cahn et al., 2014). Integration of SIMS with these and other irrigation management software tools facilitates correction for soil evaporation and crop water stress via a soil water balance model, and supports calculation of irrigation system operating-times from ET data. These tools also provide the ability to maintain records and calculate on-farm water use efficiency metrics, demonstrating the value of satellite-observations for a variety of on-farm water management applications.

7. Conclusions and recommendations

The crop coefficient methodology adopted and documented in FAO56 is a successful and essential component for improved agricultural water management and, particularly, for promoting water savings and precision irrigation. The methodology has been, and continues to be, widely used for vegetable, field and fruit crops to determine crop water requirements, assess irrigation needs and support irrigation scheduling and management throughout the world, due to both its relative simplicity and robustness. Nevertheless, the predictive estimation of K_c and K_{cb} can be challenging, with the use of tabulated values for K_c and K_{cb} being the most common option used by practitioners. However, many cropped conditions can deviate from those represented by the standardized, tabulated values due to different cropping or tree densities and agronomic practices.

Research over the past 50 years has demonstrated for a variety of vegetable, field and fruit crops that crop coefficients relate well with the leaf area index, the fraction of ground cover (f_c), the fraction of ground shaded by the canopy (f_{shad}), and the fraction of intercepted photosynthetic active radiation (f_{IPAR}). These relationships can be varied using factors that explain the variability of K_c values obtained from crop ET determined in field; however, they have not been generally used to predict K_c or K_{cb}. These relationships, reviewed in this study, nevertheless provided for a first approach adopted in FAO56 to estimate K_c from the effective f_c or LAI and the crop height (h) through relating $K_{cb\ mid}$ with LAI or f_c through the $K_{cb\ full}$, i. e., the K_{cb} during the mid-season, at peak plant height, for vegetation having full ground cover or LAI > 3. The original $K_{cb\ mid}$-LAI and $K_{cb\ mid}$-f_c equations

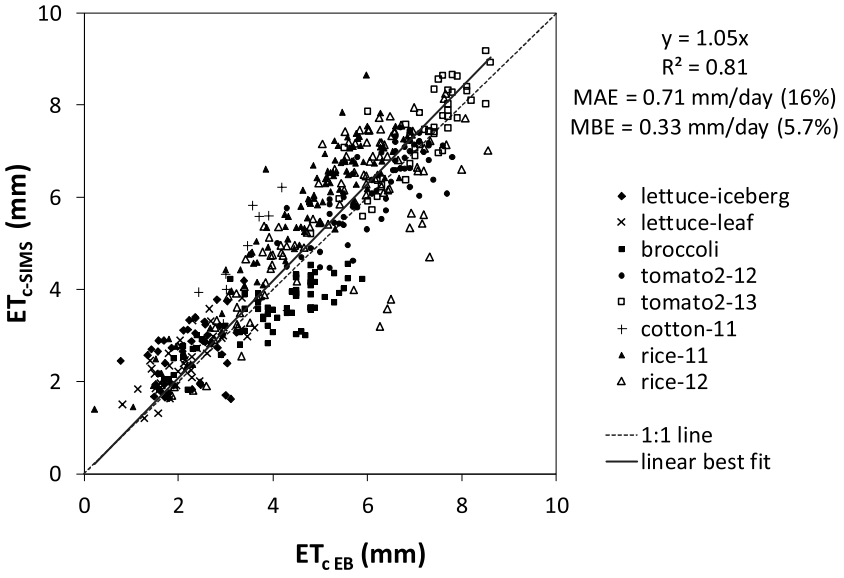

Fig. 21. Daily crop evapotranspiration derived from SIMS observations ($ET_{c\text{-}SIMS}$) plotted against ET_c obtained from ground-based energy balance measurements ($ET_{c\ EB}$) of annual crops for sites and date ranges representing well-watered conditions with $f_{c\text{-}eff} > 25\%$. Linear best fit is forced through the origin; also depicted is the 1:1 line.

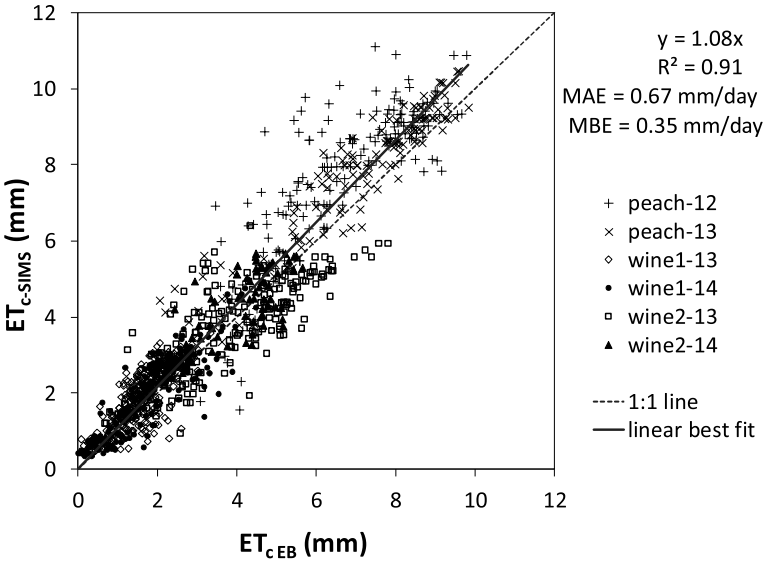

Fig. 22. Daily crop evapotranspiration derived from SIMS observations ($ET_{c\ SIMS}$) plotted against ET_c obtained from ground-based energy balance measurements ($ET_{c\ act\ EB}$) of perennial crops for sites and date ranges representing well-watered conditions with $f_{c\text{-}eff} > 25\%$. Linear best fit is forced through the origin; also depicted is the 1:1 line.

proposed in FAO56 were aimed at estimating $K_{cb\ mid}$ for natural, non-typical or non -pristine agricultural vegetation that were not included in the K_c and K_{cb} tables, and thus were not focused on the common agricultural crops. A resistance correction factor (F_r) was proposed in FAO56 to consider the effects of stomatal control by the vegetation under study. That methodology has received limited adoption despite research that has proven that strong relations exist between K_c or K_{cb} with f_c or LAI, especially for tree and vine crops. Therefore, that FAO56 approach was upgraded with the A&P approach (Allen and Pereira, 2009) through the development of a more visual density coefficient (K_d) computed either from f_c and h, or from LAI, and by adopting specific equations for crop coefficients for orchards and vineyards, including consideration of active ground cover.

The review provided here has shown good acceptance of the approach by the research community. Therefore, it is opportune to test and summarize the approach for a variety of vegetable, field and forage crops, as well as orchards and vineyards, with a focus on the parameterization of the A&P equations. Results comparing the A&P predicted K_{cb} ($K_{cb\ A\&P}$) with K_{cb} values obtained from field measurements reveal coefficients of regression close to 1.0, indicating that $K_{cb\ A\&P}$ values are statistically close to those obtained from field data, and with RMSE generally smaller than 10 % of K_{cb}, often not exceeding 5 %. The accurate results obtained allow us to conclude that the A&P approach is appropriate to use for estimating crop coefficients from observed crop characteristics like f_c and h. A recently proposed modification of the stomatal resistance adjustment parameter F_r for apple orchards (Mobe et al., 2020) opens a new area of research for orchards when leaf resistances are observed.

Observing crop heights is easy but determining average f_c in the field over large areas can be challenging and requires appropriate methods. Different approaches are reviewed herein and particular attention is paid to determining f_c from remote sensing. In line with this, a summary of results from the application of the Satellite Irrigation Management Support (SIMS) System are analyzed. The accuracy of estimating daily crop ET obtained with the A&P approach when f_c is derived from time-series of satellite measurements of NDVI ($ET_{c\text{-}SIMS}$) was compared with daily ET determined from ground-based energy balance measurements ($ET_{c\ EB}$). For annual crops, the daily mean absolute error between $ET_{c\text{-}SIMS}$ and $ET_{c\ EB}$ was MAE = 0.71 mm d^{-1} (16.0 %) and the mean bias error (MBE) was small, representing 5.7 %. The largest differences were associated with a rice crop, likely due to flood irrigation events that substantially increased evaporation even with a well-established canopy, plus impacts of exposed water on the NDVI signal. For perennial crops, MAE was also small, 0.67 mm d^{-1}, however larger in relative terms (21.7 %), while MBE represented only 6.9 %. While the field data included in the analysis only address a small fraction of the hundreds of different crops grown in California, the crops included in the analysis span a wide range of growth forms and irrigation methods. Overall, the results demonstrate the utility of the A&P approach to provide valuable information for irrigation scheduling and management that is representative of well-watered conditions.

Research on both lines needs to be continued to support both ground and satellite-based applications in irrigation scheduling and management, namely to support users in parameterizing the A&P approach with easy to obtain information. With this objective, a companion paper (Pereira et al., 2020a) tabulates K_{cb} for vegetable and field crops based on related literature reviews (Pereira et al., 2020b, c), and tabulates K_{cb} for orchards and vineyards using satellite SIMS data and reviewed ground crop data. It is our overall goal that the use of the A&P approach can contribute to water savings and more precise irrigation management, thus contributing to the increased resilience of agricultural production to climate change.

Declaration of Competing Interest

The authors declare that they have no known competing financial interests or personal relationships that could have appeared to influence the work reported in this paper.

Acknowledgements

The support of the Fundação para a Ciência e a Tecnologia, Portugal, through the research grant attributed to the research unit LEAF (UID/AGR/04129/2013) and to the second author (DL 57/2016/CP1382/CT0022) is acknowledged. R. López-Urrea and J.J. Cancela acknowledge the financial support from different Spanish ministries, as well as Castilla-La Mancha and Galicia councils throughout different projects carried out in the last 20 years, such as ongoing projects AGL2017-83738-C3-3-R and SBPLY/17/180501/000357, and from the European Commission with project “SUPROMED” (grant number 1813). Support for the satellite data analyses and collection of ground measurements was provided by the NASA Applied Sciences Program, the NASA Western Water Applications Office, the California State University Agricultural Research Institute, and the USDA National Institute of Food and Agriculture.

References

Abatzoglou, J.T., 2013. Development of gridded surface meteorological data for ecological applications and modelling. Int. J. Climatol. 33, 121–131.

Adams, J.E., Arkin, G.F., 1977. A light interception method for measuring row crop ground cover. Soil Sci. Soc. Am. J. 41, 789–792.

Adams, J.E., Arkin, G.F., Ritchie, J.T., 1976. Influence of row spacing and straw mulch on first stage drying. Soil Sci. Soc. Am. J. 40, 436–442.

Al-Kaisi, M., Brun, L.J., Enz, J.W., 1989. Transpiration and evapotranspiration from maize as related to leaf area index. Agric. For. Meteorol. 48, 111–116.

Al-Khafaf, S., Wierenga, P.J., Williams, B.C., 1978. Evaporative flux from irrigated cotton as related to leaf area index, soil water, and evaporative demand. Agron. J. 70, 912–917.

Allen, R.G., 2011. Skin layer evaporation to account for small precipitation events—an enhancement to the FAO-56 evaporation model. Agric. Water Manage. 99, 8–18.

Allen, R.G., Pereira, L.S., 2009. Estimating crop coefficients from fraction of ground cover and height. Irrig. Sci. 28, 17.

Allen, R.G., Pruitt, W.O., Businger, J.A., Fritschen, L.J., Jensen, M.E., Quinn, F.H., 1996. Evaporation and transpiration. In: Wooton, T.P., Cecilio, C.B., Fowler, L.C., Hui, S.L., Heggen, R.J. (Eds.), ASCE Handbook of Hydrology. ASCE, New York, pp. 125–252.

Allen, R.G., Pereira, L.S., Raes, D., Smith, M., 1998. Crop Evapotranspiration. Guidelines for Computing Crop Water Requirements. FAO Irrig. Drain. Pap. 56. FAO, Rome 300 p.

Allen, R.G., Pereira, L.S., Smith, M., Raes, D., Wright, J.L., 2005a. FAO-56 Dual crop coefficient method for estimating evaporation from soil and application extensions. J. Irrig. Drain. Eng. 131 (1), 2–13.

Allen, R.G., Pruitt, W.O., Raes, D., Smith, M., Pereira, L.S., 2005b. Estimating evaporation from bare soil and the crop coefficient for the initial period using common soils information. J. Irrig. Drain. Eng. 131 (1), 14–23.

Allen, R.G., Pruitt, W.O., Wright, J.L., Howell, T.A., Ventura, F., Snyder, R., Itenfisu, D., Steduto, P., Berengena, J., Baselga, J., Smith, M., Pereira, L.S., Raes, D., Perrier, A., Alves, I., Walter, I., Elliott, R., 2006. A recommendation on standardized surface resistance for hourly calculation of reference ETo by the FAO56 Penman-Monteith method. Agric. Water Manage. 81, 1–22.

Allen, R.G., Wright, J.L., Pruitt, W.O., Pereira, L.S., Jensen, M.E., 2007. Water requirements. In: Hoffman, G.J., Evans, R.G., Jensen, M.E., Martin, D.L., Elliot, R.L. (Eds.), Design and Operation of Farm Irrigation Systems, 2nd edition. ASABE, St. Joseph, MI, pp. 208–288.

Allen, R.G., Pereira, L.S., Howell, T.A., Jensen, M.E., 2011. Evapotranspiration information reporting: I. Factors governing measurement accuracy. Agric. Water Manage. 98 (6), 899–920.

Anderson, R.G., Alfieri, J.G., Tirado-Corbalá, R., Gartung, J., McKee, L.G., Prueger, J.H., Wang, D., Ayars, J.E., Kustas, W.P., 2017. Assessing FAO-56 dual crop coefficients using eddy covariance flux partitioning. Agric. Water Manage. 179, 92–102.

ASCE-EWRI, 2005. The ASCE Standardized Reference Evapotranspiration Equation. Rep. 0-7844-0805-X, ASCE Task Committee on Standardization of Reference Evapotranspiration. ASCE, Reston, VA.

Auzmendi, I., Mata, M., Lopez, G., Girona, J., Marsal, J., 2011. Intercepted radiation by apple canopy can be used as a basis for irrigation scheduling. Agric. Water Manage. 98, 886–892.

Ayars, J.E., Johnson, R.S., Phene, C.J., Trout, T.J., Clark, D.A., Mead, R.M., 2003. Water use by drip irrigated late season peaches. Irrig. Sci. 22, 187–194.

Borges, V.P., Silva, B.B., Espínola Sobrinho, J., Ferreira, R.C., Oliveira, A.D., Medeiros, J.F., 2015. Energy balance and evapotranspiration of melon grown with plastic mulch in the Brazilian semiarid region. Sci. Agric. 72 (5), 385–392.

Bryla, D.R., Trout, T.J., Ayars, J.E., 2010. Weighing lysimeters for developing crop coefficients and efficient irrigation practices for vegetable crops. HortScience 45 (11), 1597–1604.

Cahn, M., Smith, R., Hartz, T., Farrara, B., Johnson, L.F., Melton, F., 2014. Irrigation and nitrogen management decision support tool for cool season vegetables and berries. In: Proc. USCID Water Management Semi-Annual Conference (March). U.S. Committee on Irrigation and Drainage, Denver, CO. pp. 53–64.

Campos, I., Neale, C.M., López, M.-L., Balbontín, C., Calera, A., 2014. Analyzing the effect of shadow on the relationship between ground cover and vegetation indices by using spectral mixture and radiative transfer models. J. Appl. Remote Sens. 8 (1), 083562. https://doi.org/10.1117/1.JRS.8.083562.

Cancela, J.J., Fandiño, M., Rey, B.J., Martínez, E.M., 2015. Automatic irrigation system based on dual crop coefficient, soil and plant water status for *Vitis vinifera* (cv Godello and cv Mencía). Agric. Water Manage. 151, 52–63.

Cholpankulov, E.D., Inchenkova, O.P., Paredes, P., Pereira, L.S., 2008. Cotton irrigation scheduling in Central Asia: model calibration and validation with consideration of groundwater contribution. Irrig. Drain. 57, 516–532.

Cihlar, J., Dobson, M.C., Schmugge, T., Hoogeboom, P., Janse, A.R.P., Baret, F., Guyot, G., Le Toan, T., Pampaloni, P., 1987. Procedures for the description of agricultural crops and soils in optical and microwave remote sensing studies. Int. J. Remote Sens. 8, 427–439.

Conceição, N., Tezza, L., Häusler, M., Lourenço, S., Pacheco, C.A., Ferreira, M.I., 2017. Three years of monitoring evapotranspiration components and crop and stress coefficients in a deficit irrigated intensive olive orchard. Agric. Water Manage. 191, 138–152.

De la Casa, A., Ovando, G., Bressanini, L., Martínez, J., Díaz, G., Miranda, C., 2018. Soybean crop coverage estimation from NDVI images with different spatial resolution to evaluate yield variability in a plot. ISPRS J. Photogramm. Remote Sens. 146, 531–547.

Ding, R., Kang, S., Zhang, Y., Hao, X., Tong, L., Du, T., 2013. Partitioning evapotranspiration into soil evaporation and transpiration using a modified dual crop coefficient model in irrigated maize field with ground-mulching. Agric. Water Manage. 127, 85–96.

Doorenbos, J., Pruitt, W.O., 1977. Crop Water Requirements. FAO Irrigation and Drainage Paper No. 24 (rev.). FAO, Rome, Italy.

Duan, T., Zheng, B., Guo, W., Ninomiya, S., Guo, Y., Chapman, S.C., 2017. Comparison of ground cover estimates from experiment plots in cotton, sorghum and sugarcane based on images and ortho-mosaics captured by UAV. Funct. Plant Biol. 44, 169–183.

Duchemin, B., Hadria, R., Er-Raki, S., Boulet, G., Maisongrande, P., Chehbouni, A., Escadafal, R., Ezzahar, J., Hoedjes, J.C.B., Kharrou, M.H., Khabba, S., Mougenot, B., Olioso, A., Rodriguez, J.-C., Simonneaux, V., 2006. Monitoring wheat phenology and irrigation in Central Morocco: on the use of relationships between evapotranspiration, crops coefficients, leaf area index and remotely-sensed vegetation indices. Agric. Water Manage. 79, 1–27.

Er-Raki, S., Chehbouni, A., Guemouria, N., Duchemin, B., Ezzahar, J., Hadria, R., 2007. Combining FAO-56 model and ground-based remote sensing to estimate water consumptions of wheat crops in a semi-arid region. Agric. Water Manage. 87, 41–54.

Espadafor, M., Orgaz, F., Testi, L., Lorite, I.J., Villalobos, F.J., 2015. Transpiration of young almond trees in relation to intercepted radiation. Irrig. Sci. 33, 265–275.

Fan, Y., Ding, R., Kang, S., Hao, X., Du, T., Tong, L., Li, S., 2017. Plastic mulch decreases available energy and evapotranspiration and improves yield and water use efficiency in an irrigated maize cropland. Agric. Water Manage. 179, 122–131.

Fandiño, M., Cancela, J.J., Rey, B.J., Martínez, E.M., Rosa, R.G., Pereira, L.S., 2012. Using the dual-Kc approach to model evapotranspiration of albariño vineyards (*Vitis vinifera* L. cv. albariño) with consideration of active ground cover. Agric. Water Manage. 112, 75–87.

Fernández-Pacheco, D.G., Escarabajal-Henarejos, D., Ruiz-Canales, A., Conesa, J., Molina-Martínez, J.M., 2014. A digital image-processing-based method for determining the crop coefficient of lettuce crops in the southeast of Spain. Biosyst. Eng. 117, 23–34.

Ferreira, M.I., Silvestre, J., Conceição, N., Malheiro, A.C., 2012. Crop and stress coefficients in rainfed and deficit irrigation vineyards using sap flow techniques. Irrig. Sci. 30, 433–447.

Giménez, L., García-Petillo, M., Paredes, P., Pereira, L.S., 2016. Predicting maize transpiration, water use and productivity for developing improved supplemental irrigation schedules in western Uruguay to cope with climate variability. Water 8, 309. https://doi.org/10.3390/w8070309.

Giménez, L., Paredes, P., Pereira, L.S., 2017. Water use and yield of soybean under various irrigation regimes and severe water stress. Application of AquaCrop and SIMDualKc models. Water 9, 393. https://doi.org/10.3390/w9060393.

Girona, J., del Campo, J., Mata, M., Lopez, G., Marsal, J., 2011. A comparative study of apple and pear tree water consumption measured with two weighing lysimeters. Irrig. Sci. 29, 55–63.

González-Esquiva, J.M., García-Mateos, G., Hernández-Hernández, J.L., Ruiz-Canales, A., Escarabajal-Henerajos, D., Molina-Martínez, J.M., 2017. Web application for analysis of digital photography in the estimation of irrigation requirements for lettuce crops. Agric. Water Manage. 183, 136–145.

González-Talice, J., Yuri, J.A., Lepe, V., Hirzel, J., del Pozo, A., 2012. Water use in three apple cultivars from the second season to sixth season in a drainage lysimeter. Sci. Hortic-Amsterdam 146, 131–136.

Goodwin, I., Whitfield, D.M., Connor, D.J., 2003. The relationship between peach tree transpiration and effective canopy cover. Acta Hort. 664, 283–289.

Goodwin, I., Whitfield, D.M., Connor, D.J., 2006. Effects of tree size on water use of peach (*Prunus persica* L. Batsch). Irrig. Sci. 24 (2), 59–68.

Gorelick, N., Hancher, M., Dixon, M., Ilyushchenko, S., Thau, D., Moore, R., 2017. Google earth engine: planetary-scale geospatial analysis for everyone. Remote Sens. Environ. 202, 18–27.

Grattan, S., Bowers, W., Dong, A., Snyder, R., Carroll, J., George, W., 1998. New crop coefficients estimate water use of vegetable, row crops. Calif. Agric. 52, 16–21.

Hart, Q.J., Brugnach, M., Temesgen, B., Rueda, C., Ustin, S.L., Frame, K., 2009. Daily reference evapotranspiration for California using satellite imagery and weather station measurement interpolation. Civ. Eng. Environ. Syst. 26 (1), 19–33.

Heilman, J.L., Heilman, W.E., Moore, D.G., 1982. Evaluating the crop coefficient using spectral reflectance. Agron. J. 74, 967–971.

Hernández-Hernández, J.L., García-Mateos, G., González-Esquiva, J.M., Escarabajal-Henarejos, D., Ruiz-Canales, A., Molina-Martínez, J.M., 2016. Optimal color space selection method for plant/soil segmentation in agriculture. Comput. Electron. Agric. 122, 124–132.

Hernández-Hernández, J.L., Ruiz-Hernández, J., García-Mateos, G., González-Esquiva, J.M., Ruiz-Canales, A., Molina-Martínez, J.M., 2017. A new portable application for automatic segmentation of plants in agriculture. Agric. Water Manage. 183, 146–157.

Hunsaker, D.J., French, A.N., Thorp, K.R., 2013. Camelina water use and seed yield response to irrigation scheduling in an arid environment. Irrig. Sci. 31, 911–929.

Ibraimo, N.A., Taylor, N.J., Steyn, J.M., Gush, M.B., Annandale, J.G., 2016. Estimating water use of mature pecan orchards: a six stage crop growth curve approach. Agric. Water Manage. 177, 359–368.

Imukova, K., Ingwersen, J., Streck, T., 2015. Determining the spatial and temporal dynamics of the green vegetation fraction of croplands using high-resolution RapidEye satellite images. Agric. For. Meteorol. 206, 113–123.

Jensen, M.E., Allen, R.G. (Eds.), 2016. Evaporation, Evapotranspiration, and Irrigation Water Requirements, 2nd ed. ASCE Manual 70, ASCE, Reston, VI 744 p.

Jiang, X., Kang, S., Tong, L., Li, F., Li, D., Ding, R., Qiu, R., 2014. Crop coefficient and evapotranspiration of grain maize modified by planting density in an arid region of northwest China. Agric. Water Manage. 142, 135–143.

Johnson, L.F., Melton, F.S., 2017. Basal Crop Coefficient Estimation by the Density Coefficient Approach Constrained by Satellite Data. Whitepaper Draft (16 May 2017), Personal Communication.

Johnson, D., Mueller, R., 2010. The 2009 cropland data layer. Photogramm. Eng. Remote Sens. 76 (11), 1201–1205.
Johnson, L.F., Trout, T.J., 2012. Satellite NDVI assisted monitoring of vegetable crop evapotranspiration in California's San Joaquin Valley. Remote Sens. 4 (2), 439–455.
Johnson, R.S., Ayars, J., Trout, T., Mead, R., Phene, C., 2000. Crop coefficients for mature peach trees are well correlated with midday canopy light interception. Acta Hort. 537, 455–460.
Johnson, L.F., Cassel-Sharma, F., Goorahoo, D., Melton, F., 2014. Calculator for evaluation of crop water use fractions in California. In: AGU Fall Meeting. 15–19 December, San Francisco. (#H41E-0868).
Linquist, B., Snyder, R., Anderson, F., Espino, L., Inglese, G., Marras, S., Moratiel, R., Mutters, R., Nicolosi, P., Rejmanek, H., Russo, A., 2015. Water balances and evapotranspiration in water-and dry-seeded rice systems. Irrig. Sci. 33 (5), 375–385.
López-López, M., Espadafor, M., Testi, L., Lorite, I.J., Orgaz, F., Fereres, E., 2018. Water requirements of mature almond trees in response to atmospheric demand. Irrig. Sci. 36 (4-5), 271–280.
López-Urrea, R., Martín de Santa Olalla, F., Montoro, A., López-Fuster, P., 2009a. Single and dual crop coefficients and water requirements for onion (*Allium cepa* L.) under semiarid conditions. Agric. Water Manage. 96, 1031–1036.
López-Urrea, R., Montoro, A., González-Piqueras, J., López-Fuster, P., Fereres, E., 2009b. Water use of spring wheat to raise water productivity. Agric. Water Manage. 96, 1305–1310.
López-Urrea, R., Montoro, A., Mañas, F., López-Fuster, P., Fereres, E., 2012. Evapotranspiration and crop coefficients from lysimeter measurements of mature 'Tempranillo' wine grapes. Agric. Water Manage. 112, 13–20.
López-Urrea, R., Montoro, A., Trout, T.J., 2014. Consumptive water use and crop coefficients of irrigated sunflower. Irrig. Sci. 32 (2), 99–109.
López-Urrea, R., Martínez-Molina, L., de la Cruz, F., Montoro, A., González-Piqueras, J., Odi-Lara, M., Sánchez, J.M., 2016. Evapotranspiration and crop coefficients of irrigated biomass sorghum for energy production. Irrig. Sci. 34, 287–296.
Lozano, D., Ruiz, N., Gavilán, P., 2016. Consumptive water use and irrigation performance of strawberries. Agric. Water Manage. 169, 44–51.
Marsal, J., Girona, J., Casadesus, J., Lopez, G., Stöckle, C.O., 2013. Crop coefficient (Kc) for apple: comparison between measurements by a weighing lysimeter and prediction by CropSyst. Irrig. Sci. 31 (3), 455–463.
Martinez-Cob, A., Faci, J.M., Blanco, O., Medina, E.T., Suvočarev, K., 2014. Feasibility of using pyranometers for continuous estimation of ground cover fraction in table grape vineyards. Span. J. Agric. Res. 12, 603–610.
Martins, J.D., Rodrigues, G.C., Paredes, P., Carlesso, R., Oliveira, Z.B., Knies, A.E., Petry, M.T., Pereira, L.S., 2013. Dual crop coefficients for maize in southern Brazil: model testing for sprinkler and drip irrigation and mulched soil. Biosyst. Eng. 115, 291–310.
Medeiros, G.A., Arruda, F.B., Sakai, E., Fujiwara, M., 2001. The influence of crop canopy on evapotranspiration and crop coefficient of beans (*Phaseolus vulgaris* L.). Agric. Water Manage. 9 (3), 211–224.
Medeiros, G.A., Daniel, L.A., Fengler, F.H., 2016. Growth, development, and water consumption of irrigated bean crop related to growing degree-days on different soil tillage systems in Southeast Brazil. Int. J. Agron ID 8065985.
Melton, F.S., Johnson, L.F., Lund, C.P., Pierce, L.L., Michaelis, A.R., Hiatt, S.H., Guzman, A., Adhikari, D.D., Purdy, A.J., Rosevelt, C., Votava, P., Trout, T.J., Temesgen, B., Frame, K., Sheffner, E.J., Nemani, R.R., 2012. Satellite Irrigation Management Support with the Terrestrial Observation and Prediction System: a framework for integration of satellite and surface observations to support improvements in agricultural water resource management. IEEE J. Stars 5 (6), 1709–1721.
Melton, F., Johnson, L.F., Guzman, A., Post, K., Wang, T., Hang, M., Zaragosa, I., Temesgen, B., Trezza, R., Cahn, M., Pereira, L.S., 2020. The Satellite Irrigation Management Support (SIMS) System: satellite mapping of crop coefficients to support advances in irrigation management in California. Remote Sens. Environ (Submitted).
Miao, Q., Rosa, R.D., Shi, H., Paredes, P., Zhu, L., Dai, J., Gonçalves, J.M., Pereira, L.S., 2016. Modeling water use, transpiration and soil evaporation of spring wheat–maize and spring wheat–sunflower relay intercropping using the dual crop coefficient approach. Agric. Water Manage. 165, 211–229.
Minhas, P.S., Ramos, T.B., Ben-Gal, A., Pereira, L.S., 2020. Coping with salinity in irrigated agriculture: crop evapotranspiration and water management issues. Agric. Water Manage. 227, 105832.
Mobe, N.T., Dzikiti, S., Zirebwa, S.F., Midgley, S.J.E., von Loeper, W., Mazvimavi, D., Ntshidi, Z., Jovanovic, N.Z., 2020. Estimating crop coefficients for apple orchards with varying canopy cover using measured data from twelve orchards in the Western Cape Province, South Africa. Agric. Water Manage. 233, 106103.
Monteith, J.L., 1965. Evaporation and environment. Symposia of the Society for Experimental Biology 19. Cambridge University Press, Cambridge, pp. 205–234.
Monteith, J.L., 1981. Evaporation and surface temperature. Q. J. R. Meteorol. Soc. 107, 1–27.
Montoro, A., Mañas, F., López-Urrea, R., 2016. Transpiration and evaporation of grapevine, two components related to irrigation strategy. Agric. Water Manage. 177, 193–200.
Paço, T.A., Ferreira, M.I., Rosa, R.D., Paredes, P., Rodrigues, G.C., Conceição, N., Pacheco, C.A., Pereira, L.S., 2012. The dual crop coefficient approach using a density factor to simulate the evapotranspiration of a peach orchard: SIMDualKc model versus eddy covariance measurements. Irrig. Sci. 30, 115–126.
Paço, T.A., Pôças, I., Cunha, M., Silvestre, J.C., Santos, F.L., Paredes, P., Pereira, L.S., 2014. Evapotranspiration and crop coefficients for a super intensive olive orchard. An application of SIMDualKc and METRIC models using ground and satellite observations. J. Hydrol. 519, 2067–2080.
Paço, T.A., Paredes, P., Pereira, L.S., Silvestre, J., Santos, F.L., 2019. Crop coefficients and transpiration of a super intensive Arbequina olive orchard using the dual Kc approach and the Kcb computation with the fraction of ground cover and height. Water 11, 383. https://doi.org/10.3390/w11020383.
Paredes, P., Rodrigues, G.C., Alves, I., Pereira, L.S., 2014. Partitioning evapotranspiration, yield prediction and economic returns of maize under various irrigation management strategies. Agric. Water Manage. 135, 27–39.
Paredes, P., Pereira, L.S., Rodrigues, G.C., Botelho, N., Torres, M.O., 2017. Using the FAO dual crop coefficient approach to model water use and productivity of processing pea (*Pisum sativum* L.) as influenced by irrigation strategies. Agric. Water Manage. 189, 5–18.
Paredes, P., Rodrigues, G.J., Petry, M.T., Severo, P.O., Carlesso, R., Pereira, L.S., 2018. Evapotranspiration partition and crop coefficients of Tifton 85 Bermudagrass as affected by the frequency of cuttings. Application of the FAO56 dual Kc model. Water 10, 558. https://doi.org/10.3390/w10050558.
Pereira, L.S., Alves, I., 2013. Crop Water Requirements, Reference Module in Earth Systems and Environmental Sciences. Elsevier. https://doi.org/10.1016/B978-0-12-409548-9.05129-0.
Pereira, L.S., Perrier, A., Allen, R.G., Alves, I., 1999. Evapotranspiration: review of concepts and future trends. J. Irrig. Drain. Eng. 125 (2), 45–51.
Pereira, L.S., Paredes, P., Rodrigues, G.C., Neves, M., 2015. Modeling malt barley water use and evapotranspiration partitioning in two contrasting rainfall years. Assessing AquaCrop and SIMDualKc models. Agric. Water Manage. 159, 239–254.
Pereira, L.S., Paredes, P., López-Urrea, R., Hunsaker, D.J., Mota, M., Mohammadi Shad, Z., 2020a. Standard single and basal crop coefficients for vegetable crops, an update of FAO56 crop water requirements approach. Agric. Water Manage. https://doi.org/10.1016/j.agwat.2020.106196. (this Special Issue).
Pereira, L.S., Paredes, P., Hunsaker, D.J., López-Urrea, R., Mohammadi Shad, Z., 2020b. Standard single and basal crop coefficients for field crops. Updates and advances to the FAO56 crop water requirements method. Agric. Water Manage (submitted, this Special Issue).
Pereira, L.S., Paredes, P., Mota, M., Melton, F., Wang, T., Johnson, L., 2020c. Prediction of crop coefficients from fraction of ground cover and height. Indicative K_c and K_{cb} values for vegetable, field and fruit crops. Agric. Water Manage (submitted, this Special Issue).
Picón-Toro, J., González-Dugo, V., Uriarte, D., Mancha, L.A., Testi, L., 2012. Effects of canopy size and water stress over the crop coefficient of a "Tempranillo" vineyard in south-western Spain. Irrig. Sci. 30, 419–432.
Pôças, I., Paço, T.A., Paredes, P., Cunha, M., Pereira, L.S., 2015. Estimation of actual crop coefficients using remotely sensed vegetation indices and soil water balance modelled data. Remote Sens. 7 (3), 2373–2400.
Puppo, L., García, C., Bautista, E., Hunsaker, D.J., Beretta, A., Girona, J., 2019. Seasonal basal crop coefficient pattern of young non-bearing olive trees grown in drainage lysimeters in a temperate sub-humid climate. Agric. Water Manage. 226, 105732.
Qiu, R., Song, J., Du, T., Kang, S., Tong, L., Chen, R., Wu, L., 2013. Response of evapotranspiration and yield to planting density of solar greenhouse grown tomato in northwest China. Agric. Water Manage. 130, 44–51.
Raes, D., Steduto, P., Hsiao, T.C., Fereres, E., 2009. AquaCrop - the FAO crop model to simulate yield response to water: II. Main algorithms and software description. Agron. J. 101, 438–447.
Ritchie, J.T., 1972. Model for predicting evaporation from a row crop with incomplete cover. Water Resour. Res. 8 (5), 1204–1213.
Ritchie, J.T., Burnett, E., 1971. Dryland evaporative flux in a subhumid climate: III. Plant influences. Agron. J. 63, 56–62.
Rosa, R.D., 2019. Modelação da evapotranspiração com o modelo SIMDualKc: Aplicação à rega de fruteiras, a consociações de culturas e a condições salinas, e ligação ao SIG para análise à escala do projecto de rega. PhD. Thesis. Instituto Superior de Agronomia, Universidade de Lisboa.
Rosa, R.D., Paredes, P., Rodrigues, G.C., Fernando, R.M., Alves, I., Pereira, L.S., Allen, R.G., 2012a. Implementing the dual crop coefficient approach in interactive software. 1. Background and computational strategy. Agric. Water Manage. 103, 8–24.
Rosa, R.D., Paredes, P., Rodrigues, G.C., Alves, I., Fernando, R.M., Pereira, L.S., Allen, R.G., 2012b. Implementing the dual crop coefficient approach in interactive software. 2. Model testing. Agric. Water Manage. 103, 62–77.
Rosa, R., Ramos, T., Pereira, L.S., 2016. The dual Kc approach to assess maize and sweet sorghum transpiration and soil evaporation under saline conditions. Application of the SIMDualKc model. Agric. Water Manage. 177, 77–94.
Samani, Z., Bawazir, S., Skaggs, R., Longworth, J., Piñon, A., Tran, V., 2011. A simple irrigation scheduling approach for pecans. Agric. Water Manage. 98, 661–664.
Sánchez, J.M., López-Urrea, R., Rubio, E., González-Piqueras, J., Caselles, V., 2014. Assessing crop coefficients of sunflower and canola using two-source energy balance and thermal radiometry. Agric. Water Manage. 137, 23–29.
Sánchez, J.M., López-Urrea, R., Doña, C., Caselles, V., González-Piqueras, J., Niclós, R., 2015. Modeling evapotranspiration in a spring wheat from thermal radiometry: crop coefficients and E/T partitioning. Irrig. Sci. 33, 399–410.
Santos, C., Lorite, I.J., Allen, R.G., Tasumi, M., 2012. Aerodynamic parameterization of the satellite-based energy balance (METRIC) model for ET estimation in rainfed olive orchards of Andalusia, Spain. Water Resour. Manage. 26 (11), 3267–3283.
Semmens, K.A., Anderson, M.C., Kustas, W.P., Gao, F., Alfieri, J.G., McKee, L., Prueger, J.H., Hain, C.R., Cammalleri, C., Yang, Y., Xia, T., 2016. Monitoring daily evapotranspiration over two California vineyards using Landsat 8 in a multi-sensor data fusion approach. Remote Sens. Environ. 185, 155–170.
Steduto, P., Hsiao, T.C., Raes, D., Fereres, E., 2009. AquaCrop—the FAO crop model to simulate yield response to water: I. Concepts and underlying principles. Agron. J. 101, 426–437.
Tanner, C.B., Jury, W.A., 1976. Estimating evaporation and transpiration from a row crop during incomplete cover. Agron. J. 68, 239–243.
Taylor, N.J., Mahohoma, W., Vahrmeijer, J.T., Gush, M.B., Allen, R.G., Annandale, J.G., 2015. Crop coefficient approaches based on fixed estimates of leaf resistance are not

appropriate for estimating water use of citrus. Irrig. Sci. 33, 153–166.
Trout, T.J., DeJonge, K.C., 2018. Crop water use and crop coefficients of maize in the Great Plains. J. Irrig. Drain. Eng. 144 (6), 04018009. https://doi.org/10.1061/(ASCE)IR.1943-4774.0001309.
Trout, T.J., Johnson, L.F., Gartung, J., 2008. Remote sensing of canopy cover in horticultural crops. HortScience 43 (2), 333–337.
Villalobos, F.J., Fereres, E., 1990. Evaporation measurements beneath corn, cotton, and sunflower. Agron. J. 82, 1153–1159.
Wei, Z., Paredes, P., Liu, Y., Chi, W.W., Pereira, L.S., 2015. Modelling transpiration, soil evaporation and yield prediction of soybean in North China Plain. Agric. Water Manage. 147, 43–53.
Williams, L.E., Ayars, J.E., 2005. Grapevine water use and the crop coefficient are linear functions of the shaded area measured beneath the canopy. Agric. Forest Meteorol. 132, 201–211.
Wu, Y., Liu, T., Paredes, P., Duan, L., Pereira, L.S., 2015a. Water use by a groundwater dependent maize in a semi-arid region of Inner Mongolia: evapotranspiration partitioning and capillary rise. Agric. Water Manage. 152, 222–232.
Wu, Y., Liu, T., Paredes, P., Duan, L., Wang, H., Wang, T., Pereira, L.S., 2015b. Ecohydrology of groundwater-dependent grasslands of the semi-arid Horqin sandy land of Inner Mongolia focusing on evapotranspiration partition. Ecohydrology 9, 1052–1067.
Zhang, B., Liu, Y., Xu, D., Zhao, N., Lei, B., Rosa, R.D., Paredes, P., Paço, T.A., Pereira, L.S., 2013. The dual crop coefficient approach to estimate and partitioning evapotranspiration of the winter wheat - summer maize crop sequence in North China Plain. Irrig. Sci. 31, 1303–1316.
Zhang, H., Anderson, R.G., Wang, D., 2015. Satellite-based crop coefficient and regional water use estimates for Hawaiian sugarcane. Field Crops Res. 180, 143–154.
Zhang, D., Mansaray, L.R., Jin, H., Sun, H., Kuang, Z., Huang, J., 2018. A universal estimation model of fractional vegetation cover for different crops based on time series digital photographs. Comput. Electron. Agric. 151, 93–103.
Zhao, N., Liu, Y., Cai, J., Paredes, P., Rosa, R.D., Pereira, L.S., 2013. Dual crop coefficient modelling applied to the winter wheat - summer maize crop sequence in North China Plain: basal crop coefficients and soil evaporation component. Agric. Water Manage. 117, 93–105.
Zhao, P., Kang, S., Li, S., Ding, R., Tong, L., Du, T., 2018. Seasonal variations in vineyard ET partitioning and dual crop coefficients correlate with canopy development and surface soil moisture. Agric. Water Manage. 197, 19–33.
Zheng, J., Huang, G., Jia, D., Wang, J., Mota, M., Pereira, L.S., Huang, Q., Xu, X., Liu, H., 2013. Responses of drip irrigated tomato (*Solanum lycopersicum* L.) yield, quality and water productivity to various soil matric potential thresholds in an arid region of Northwest China. Agric. Water Manage. 129, 181–193.